ANGEWANDTE CHEMIE © WILEY-VCH

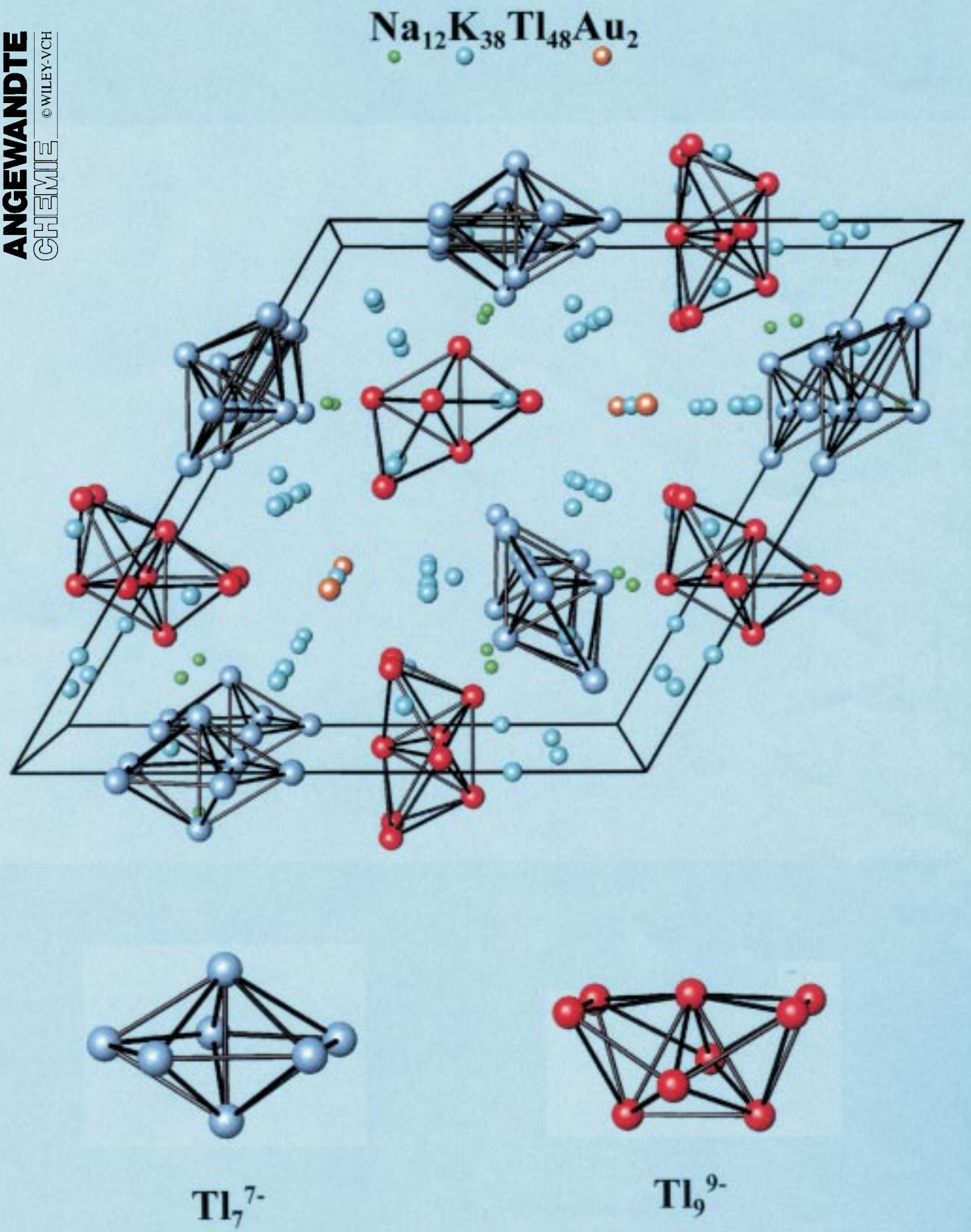

An alkali metal – thallium – gold phase with complex anionic thallium clusters

Polyanionic Clusters and Networks of the Early p-Element Metals in the Solid State: Beyond the Zintl Boundary

John D. Corbett*

Dedicated to Professor Arndt Simon on the occasion of his 60th Birthday

Reduction of p-element (post-transition) metals and metalloids by alkali metals leads to many salts containing polyatomic clusters or network anions of these elements. The earliest solvated examples were referred to as Zintl ions. Synthetic explorations have now established that many of the clusters can in fact be obtained from neat (solvent free) high-temperature reactions of binary to quaternary systems, particularly for the heavier tetrel (group 14) and triel (group 13) elements. Some synthetic tricks have also proven useful. Electronic guidelines such as Wade's rules, known to account well for other types of electron-deficient cluster bonding, are widely applicable to these compounds, but numerous hypoelectronic (electron-poor) trielide salts have also been discovered. These developments also extend to related infinite network structures and Zintl (valence) compounds. The Zintl boundary designation traditionally delineated the tetrel elements that form salts with the active metals from those of the triel and earlier elements that were once thought to generate only intermetallic phases. The distinction no longer seems appropriate, at least with regard to some alkali-metal compounds of the triel elements.

It is always difficult to predict the unimaginable

1. Introduction

A great deal is known and understood about metal–metal bonding of the transition metals in well-reduced systems, both as ligated clusters and in extended solids; the number and variety of examples arising in large part because many good bonding d orbitals are available. An analogous chemistry for the pretransition metals appears to be precluded by their diffuse orbitals and weak metal–metal bonds, although the novel delocalized bonding about simple anions in a few metal-rich arrays characterized by Simon is a unique feature of alkali-metal chemistry.[1] The chemistry of the alkaline-earth metals (including magnesium) seems to be unusually bereft of significant metal–metal bonding features beyond the elements themselves and a few nitride compounds. In contrast, the comparative metal–metal bonding among compounds of the main group p-metals (metametals, metalloids) with the active metals is widespread and anomalous with regard to traditional examples. On the other hand, aluminum chemistry in intermetallic systems does not correlate well with catenation characteristics of the other p-metals, although this element does show a remarkable solid-state chemistry of its own. Thus, another classification for this review could be in terms of the cluster and network chemistry of the post-transition elements. In this regard there is still little basis for the separation of silicon from germanium chemistry.

The post-transition metals are themselves highly irregular or nonclassical in terms of structures and properties and are often not considered as "real" metals.[2, 3] Compounds of the heavier p-metals also tend to be relatively electron-poor, to the degree that the ns^2 pairs act increasingly corelike in reduced phases. Perhaps something unusual should have been anticipated with respect to their element–element bonding (catenation) in the electron-richer systems, but as it was not, a surprising length of time passed before these features were discovered or generally recognized. Catenation is, of course, well known for boron, carbon, silicon, and so forth. Indeed, elementary views of the bonding in clusters of the heavier metal analogues in Zintl phases and ions (see below) are based on precepts similar to those developed for the nonmetals—namely, Wade's and the octet rules. The former were the first to organize in an empirical manner the compositions, electron counts, and geometries arising with the delocalized electron-deficient cluster bonding in the boron hydrides and boranes,[4] which in fact have clear and functional parallels in

[*] Prof. J. D. Corbett
Department of Chemistry and Ames Laboratory
Iowa State University
Ames, IA 50011 (USA)
Fax: (+1) 515-294-5718
E-mail: jdc@ameslab.gov, jcorbett@iastate.edu

  1433-7851/00/3904-0671 $ 17.50+.50/0

"naked" clusters of the heavy p-metals because of the increasing inertness or energetic isolation of the ns^2 pairs.[5]

The applicability of the octet rule and the occurrence of anionic, homoatomic analogues of some catenated nonmetals were first recognized among alkali-metal "salts" of the heavy metals and metalloids. Such salts are now often termed Zintl (or Zintl–Klemm) or valence phases (broadly expanded to include modern bonding concepts),[6–11] while polyanions of the heavier metals, once known only in solution with liquid ammonia, are termed Zintl ions.[11, 12] The further distinction of the Zintl boundary (or Zintl border) was introduced by Laves[6, 11] as the dividing line between what we chose to call the triel group (group 13, aluminum or gallium family, symbol Tr) and the tetrel group (group 14, silicon family, symbol Tt).[13] The border itself had been defined earlier by Zintl[14] as the left-hand limit on the periodic table for elements that allow the formation of 1) monoatomic (8-*N*) anions (Sb^{3-}, Sn^{4-},...) in saltlike structures of compounds richest in an active metal (for example Mg_2Sn in the anti-(CaF_2) structure family) as opposed to alloylike phases,[13] and 2) polyanions under strongly reducing conditions in liquid ammonia that were later designated[15] as Zintl ions. All assignments of Zintl's name to these categories occurred posthumously.

In this article we relate the considerable amount of new chemistry that has been discovered for the earlier p-metals within the last 25 years, with emphasis on the newer developments in the solid state. A review of similar material appeared in 1996.[16]

2. Traditional Zintl Ions

In the 1930s, Zintl provided the first substantial characterizations of what became termed Zintl ions, although fragmentary evidence regarding the unusual green solutions of lead metal (or its halides) when treated with sodium solutions in liquid ammonia had been known since the 1890s. As reviewed earlier,[12] his extensive studies led to empirical formulae for a variety of what appeared to be polyanionic salts of the post-transition metals in liquid ammonia, for example Sn_9^{4-}, Pb_9^{4-}, Pb_7^{4-}, Sb_3^{3-}, Bi_5^{3-}, Bi_7^{3-}. Alkaline-earth metals did not afford this chemistry, nor did the potential cluster-forming elements (Ge, Si, Ga, In, or Tl) when introduced with alkali metals (hereafter noted as A in formulae). However, none of the salts with ammoniated cations was sufficiently stable to yield crystalline products at room temperature. A few Zintl anions were isolated much later as ethylenediamine (en) complexes of the sodium salts according to analytical results, but only an incomplete crystal structure was achieved for $Na_4(en)_7Sn_9$.[17] The first general route to the isolation of salts of the Zintl anions was accomplished through provision of a stronger chelating agent for the cations, especially [2.2.2]cryptand ("crypt"). We will see later that many of these "ionic" tetrelide clusters, as well as new trielide examples, have in fact been isolated recently as neat binary compounds with the alkali metals, which are closer to the emphasis intended in this article.

2.1. Alkali Metal–Cryptand Salts of Zintl Ions

An updated list of the polyanions isolated from solution and structurally characterized, generally as complexes with cationic sodium or potassium encapsulated in [2.2.2]cryptand, is given in Table 1. (Note that what we list for all of these examples are oxidation state assignments and not the real

Table 1. Zintl anions isolated from molecular solvents with alkali-metal–cryptand cations.

Ion	Symmetry[a]	Skeletal p-electrons	Reference
Sb_4^{2-}, Bi_4^{2-}	D_{4h} (arachno)	$2n+6$	[18, 19]
$Sn_2Bi_2^{2-}$, $Pb_2Sb_2^{2-}$, $InBi_3^{2-}$	$\sim T_d$ (nido)	$2n+4$	[20–22]
Sn_5^{2-}, Pb_5^{2-}, Ge_5^{2-}	$\sim D_{3h}$ (closo)	$2n+2$	[23, 24]
Ge_9^{2-} [b]	$\sim D_{3h}$ (closo)	$2n+2$	[25]
Ge_9^{2-} [c]	$\sim C_{2v}$ (closo)	$2n+2$	[26]
Ge_9^{4-} [c]	$\sim C_{4v}$ (nido)	$2n+4$	[26]
Ge_9^{3-}	$\approx C_{2v}$	$2n+1$	[27–29]
Ge_{18}^{6-}	$\sim C_{2h}$ (dimer)	$2n+6$	[22]
Sn_9^{3-}	D_{3h} (closo)	$2n+1$	[30, 31]
Sn_9^{4-}, $In_4Bi_5^{3-}$	C_{4v} (nido)	$2n+4$	[22, 32]
$_\infty^1[KSn_9^{3-}]$, $_\infty^1[KPb_9^{3-}]$	$\sim C_{4v}+K^+$ (chains)	$2n+4$	[33, 34]
Pb_9^{3-}	$\approx C_{2v}$	$2n+1$	[28, 31, 34]
$TlSn_8^{3-}$ [c]	$\sim D_{3h}$ (closo)	$2n+2$	[35]
$TlSn_9^{3-}$ [c]	$\sim D_{4h}$ (closo)	$2n+2$	[35]

[a] Neglecting heteroatoms. [b] This structure was first reported as a disordered Ge_{10}^{2-} cluster,[36] later shown to be false upon reanalysis. [c] Double salts.

John D. Corbett, a native of the Pacific Northwest, has spent all of his professional career at Iowa State University since completing his undergraduate and graduate studies (under N. W. Gregory) at the University of Washington. He is presently Distinguished Professor in the College of Liberal Arts and Sciences as well as Professor of Chemistry and Senior Chemist in the Ames Laboratory of the US Department of Energy. His other research interests include metal–molten salt chemistry, syntheses of highly reduced compounds of the early transition metals, cluster and interstitial chemistry, and structure and bonding in the solid state. He has been an Alexander von Humboldt Senior Scientist with Professors R. Hoppe and H.-G. von Schnering, the recipient of two Department of Energy awards in Materials Chemistry and of the American Chemical Society Award in Inorganic Chemistry. He is the designee for the ACS 2000 Award for Distinguished Service in the Advancement of Inorganic Chemistry and a member of the US National Academy of Sciences.

charges.) Considerable expansion of Zintl's original list of polyanions has been possible, while others on his list have not been reproduced, or have been reformulated as other charge types. Note that, relative to the compounds formed in liquid ammonia, inclusion of the cryptand in the reactions expands the cluster-forming elements listed to include germanium, a family of paramagnetic Tt_9^{3-} ions (Tt = Ge – Pb), and a couple of substitutional examples involving some of the earlier triel elements. However, no general expansion to include elements further left in the periodic table, beyond the Zintl boundary, has been achieved by forming the complex as a cationic alkali-metal – cryptand salt.

Except for the tetrahedra listed at the beginning of Table 1, all of these polyanions are best described (on comparison with the relatively electron-rich tetrahedra P_4 and As_4) in terms of delocalized electron-deficient bonding, sometimes referred to hereafter as "classical" bonding, which is to include modern views of cluster bonding. These tetrahedra are classified further according to Wade's useful rules and their skeletal p-electron counts, as follows:[4] the *closo*-deltahedra, of n deltahedral atoms, require $2n+2$ skeletal p-electrons (specifically, Tt_n^{2-} for all tetrelide clusters); *nido* clusters, with their deltahedra missing one vertex, require $2n+4$ electrons (cluster-based electrons of the $n+1$ *closo*-parent remain); and *arachno* polyhedra, missing two vertices, require $2n+6$ electrons. Of course, the same conclusions regarding these special points of electronic stability may be readily obtained from extended Hückel molecular-orbital calculations, spherical-harmonic treatments, and so forth.[37] In most cases, the ns^2 states mix only weakly into the skeletal bonding orbitals, corresponding instead to nearly inert ns^2 cores.

The important feature is the generality of these simple guidelines for relating geometry to electron count for clusters with notable electronic stabilities. There seem to be no significant exceptions, save for some surprising radicals. A novel, dimeric product of the radical Ge_9^{3-} is shown in Figure 1a. (References will not repeated in the text or the

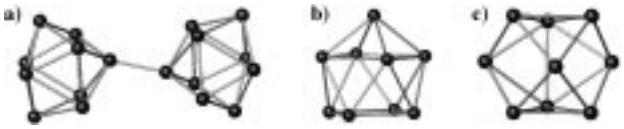

Figure 1. Examples of tetrelide anions, as [A ⊂ crypt] salts. a) Ge_{18}^{6-}, the dimer of the Ge_9^{3-} radical. The b) C_{4v} and c) $\sim D_{3h}$ pair in K_4Pb_9.

Figure captions when these references can be unambiguously found in a Table.) Most of the observed cluster symmetries given in Table 1 are in close agreement with expectations, or have recognizable relationships when characteristic proportions or dihedral angles are considered. On the other hand, the three (or more) nine-atom Tt_9^{n-} species do include geometric uncertainties because of some evident "softness", disorder of mixed species, or cavity-dependent variations, especially for $n = 2, 3$. The Tt_9^{4-} species are fairly close to the unicapped square antiprismatic (*nido*) ideal, whereas the isolated *closo*-Ge_9^{2-} and the exceptional Sn_9^{3-} radical ion are close to D_{3h} symmetry. On the other hand, the anions in A ⊂ [2.2.2]crypt salts of Ge_9^{3-}[27] and Pb_9^{3-},[28] that each contain one unique cluster, exhibit appreciable distortions from C_{2v} symmetry. Three paramagnetic $[A \subset [2.2.2]\text{cryptand}]_3Tt_9$ phases, one each for germanium,[29] tin, and lead,[31], contain pairs of independent clusters showing significant (Ge) or some (Sn, Pb) degree of distortion. However, recent reanalysis on the basis of quantitative magnetic studies shows that only one-half of the tin and lead members are paramagnetic.[38] Clear examples of Tt_9^{2-} have been limited to Ge_9^{2-}, where the first charge assignment was made on the basis of geometry alone,[26] there being at the time no reason to suspect odd numbered electron clusters. However, Ge_9^{2-} has been recently confirmed, as a cryptand salt, as a single D_{3h} anion.[25] Recently, several salts of the Sn_9^{4-} and Pb_9^{4-} ions have been obtained by direct reaction of the elements in liquid [18]crown-6.[39] These results are novel since this complexant does not completely sequester the cations, and several direct alkali-metal – cluster interactions remain.

2.2. Related Group 15 and 16 Cations

It turns out that the list of classical ions in Table 1 may be expanded to include isoelectronic and isosteric cations from electron-richer families shown in Table 2. Limiting stabilities

Table 2. Isoelectronic polycations prepared with weakly basic haloanions ($AlCl_4^-$, $HfCl_6^{2-}$).

Ion	Symmetry	Skeletal p-electrons	Reference
Se_4^{2+}, Te_4^{2+}	D_{4h}	$2n+6$ (arachno)	[40, 41]
Bi_5^{3+}	D_{3h}	$2n+2$ (closo)	[42, 43]
Bi_8^{2+}	$\sim D_{4d}$	$2n+6$ (arachno)	[42, 44]
Bi_9^{5+}	D_{3h}	$2n+4$ (closo)	[45]

of these cations are now defined by the disproportionation reactions to the elements and higher oxidation state compounds, and these reactions are characteristically affected by interactions of the latter with any counteranions present. Accordingly, weakly basic anions are useful for stabilizing the polycations, for instance $AlCl_4^-$ and $HfCl_6^{2-}$, but also fluorinated anions and the like that have analogous importance in superacid systems.[46] One obvious difference between the anions (Table 1) and cations (Table 2) is the geometric contrast between the conforming unicapped square antiprism of the 22-electron *nido* anion (e.g. Sn_9^{4-}) and the tricapped trigonal prism (D_{3h}) found for the isoelectronic *closo*-Bi_9^{5+}. In fact, the latter structure is an important alternative to the *nido* geometry for a nine atom, 22-electron species, where it has been shown to arise via a 15 – 20% trigonal elongation from the ideal 20-electron D_{3h} cluster unit, a distortion that stabilizes what is otherwise the a_2'' LUMO.[30, 47]

2.3. Polytetrelide Anions in Neat Salts

Contrary to the "end of the story" implications of the results shown in Table 1, numerous "neat" salts between "naked" cations and these cluster anions have been shown to exist in the past few years; that is, salts without an added

complexant or solvent. Furthermore, these salts reveal not only numerous new classical and hypoelectronic cluster anions of the trielides (gallium family) but also emphasize the significant increase in stability achieved with tightly packed naked cations over salts with large, complexed cations. The same conditions have more recently been shown to apply to a notable number of the traditional tetrelide (Zintl ion) clusters too. (So far, virtually only the alkali-metal systems have been explored.) Thus, with modern definitions of closed-shell bonding in electron-deficient clusters, we have converged on the common classification of these neat salts of former Zintl ions as Zintl phases, solid state compounds with closed-shell bonding that have characteristics of conventional salts (Section 5). The increased stability of these species—witness the trielide members to be discussed in Section 3—is usually associated with the additional Madelung (electrostatic potential) energy realized with the tighter packing and specific interactions between the alkali-metal cations and the Zintl anions. In fact, it has been known since the early 1960s that the neat 1:1 alkali-metal:tetrelide binary phases (with the exception of lithium) are all stable and that these contain Tt_4^{4-} ions isoelectronic with P_4, As_4, and the like.[9] At the time, the relatively high charge per atom in these anions made this differentation of Zintl ions and phases reasonable and selective. On the other hand, there is still no evidence that these Tt_4^{4-} tetrahedral species can be extracted into molecular solvents under any conditions, and so these remained as a handful of examples of neat tetrelide salts for many years.

Substantial advancements regarding other tetrelide clusters have taken place recently (Table 3). The accepted view that Zintl ions of the type Tt_9^{4-} could be obtained only via reactive solution of unrelated intermetallic or alloy phases into molecular solvents has been disproven by the Sevov group for all examples. Instead, the A_4Tt_9 compounds or the related $A_{12}Tt_{17}$ species $[= (A^+)_{12}Tt_9^{4-}(Tt_4^{4-})_2]$ with the naked cations (A = K–Cs) are preparable as binary alkali-metal salts by a conventional high-temperature synthesis in tantalum vessels. The absence of an earlier recognition of these neat phases evidently arose from a lack of careful attention to the synthesis and characterization of the solid binary "alloys" and, probably, because of their very poor X-ray diffraction characteristics. Single crystal characterization was first obtained for $Rb_{12}Si_{17}$, while powder diffraction data showed that the isostructural $Cs_{12}Si_{17}$, $A_{12}Sn_{17}$ (A = K–Cs), $Rb_{12}Pb_{17}$, and $Cs_{12}Pb_{17}$ also exist.[52] Three other A_4Tt_9 structures are also known. The overall implications are that the earlier solution-state results for the Tt_9^{4-} Zintl ions and subsequent isolation as cryptand derivatives (Table 1) probably came about through the simple solution of one or another of their rather conventional salts. Of course, intercluster or cluster–alloy reactions may have also contributed to the cryptand products. Presently, evidence suggests that most other species (Tt_9^{3-} and Tt_9^{2-} in Table 1) probably originated with redox processes in solution.

Table 3. Classical[a] anionic clusters of the tetrel elements (Tt) that are stable as neat salts.

Ion	Compound	Cluster symmetry[a]	Skeletal p-electrons	Reference
Tt_4^{4-}	ATt (A = Na–Cs, Tt = Si–Pb)	T_d (*nido*)	$2n+4$	[9]
	$BaSi_2$, Na_2BaTt_2 (Tt = Si, Ge)	T_d (*nido*)	$2n+4$	[48, 49]
$TlSn_3^{5-}$	Na_5TlSn_3	T_d (*nido*)	$2n+4$	[50]
Si_9^{4-}	$A_{12}Tt_9(Tt_4)_2$ (A = Rb, Cs)	$\sim C_{4v}$ + three distorted	$2n+4$	[51]
Sn_9^{4-}	$A_{12}Tt_9(Tt_4)_2$ (A = K–Cs)	four unique clusters	$2n+4$	[52]
Ge_9^{4-}	A_4Ge_9 (A = Rb, Cs)	C_{4v} (*nido*)	$2n+4$	[53]
Pb_9^{4-}	Cs_4Pb_9	C_{4v} (*nido*)	$2n+4$	[54]
	K_4Pb_9, Rb_4Pb_9	$\sim D_{3h}$ and C_{4v} (two types)	22	[55, 56]
	$A_{12}Pb_9(Pb_4)_2$ (A = Rb, Cs)	$\sim C_{4v}$	$2n+4$	[52]
$ZnGe_8^{6-}$[b]	Cs_6ZnGe_8	$\sim D_{3h}$		[57]
$Cd_3Pb_{16}^{10-}$[b]	K_6CdPb_8	C_{2h} oligomers + Pb_4^{4-}		[58]

[a] Following Wade's rules or equivalent. [b] Not traditional deltahedra.

Of course, some vagaries of cluster conformation remain. The Si_9^{4-} clusters in monoclinic $Rb_{12}Si_{17}$ occur in four independent asymmetric forms, presumably because of packing effects. One is very close to the characteristic C_{4v} configuration, with one square face defining the base of the unicapped square antiprism, while the other three are similar but more complex. Each of the latter have *two* open "square" bases (contrast Pb_9^{4-} in Figure 1b), one diagonal thereon corresponding to an elongated prismatic edge of the alternative D_{3h} tricapped trigonal prism. Extended-Hückel MO calculations give similar large HOMO–LUMO gaps for all four configurations, while the three distorted members all have LUMOs that are similar to the extra a_2'' HOMO orbital in Bi_9^{5+}.

The first neat phase discovered was tetragonal Cs_4Ge_9, which contains four independent cluster anions as well, but these are all very similar C_{4v} examples, virtually the same as found for one cluster in the double-cluster phase $[K \subset crypt]_6(Ge_9)_2$. The cesium compound is diamagnetic, ruby-red, and semitransparent. Another is the monoclinic Cs_4Pb_9 with a single cluster that is unambiguously a unicapped square antiprism.

Discoveries of C_{4v}-symmetric Tt_9^{4-} clusters as neat alkali-metal phases are perhaps still exceeded in impact by the elucidation of the structure of diamagnetic K_4Pb_9 and Rb_4Pb_9, which contains *both* problematic configurations for Pb_9^{4-}—one as a capped antiprism of C_{4v} symmetry, the other an approximately trigonal prism (D_{3h}); see Figure 1b, c. Heretofore, the dichotomy involving these two configurations was spread between two examples: the first are the C_{4v} Tt_9^{4-} anions in binary or alkali-metal–cryptand systems; the second like the D_{3h} Bi_9^{5+} cation, known only in the presence of acidic anions such as $HfCl_6^{2-}$,[45] but distorted to C_{2v} symmetry with $BiCl_5^{2-}$ and $Bi_2Cl_8^{2-}$.[59] The choice of views can be critical in distinguishing between these configurations, and distance and dihedral angle considerations are the best means; especially useful considerations are the equal heights of the ideal trigonal prism versus the two equal diagonals and planarity of the capped and open faces of the antiprism. The shape of one Pb_9^{4-} member in K_4Pb_9 (Figure 1b) is very close to that in the $^1_\infty[KPb_9^{3-}]$ cryptand compound (C_{4v} symmetry)[34] whereas the C_{2v} version is clearly closer to the two

examples of Bi_9^{5+}. (Specifically, the divergence from the ideal for the $\sim D_{3h}$ member are $5^\circ - 9^\circ$ in two dihedral angles and two prism edges (not drawn in the Figure) are 12% longer (0.54 Å) than the third. The angular measures compare with 20°, 22°, and 28° deviations from those parameters of the antiprism.) The Rb_4Ge_9 has also been shown to take up ethylenediamine to give a $Rb_4Ge_9 \cdot en$ structure in which the cations have been partially solvated but not separated from the anion environment.[60]

It should be noted that additional evidence for Ge_9^{4-} and Sn_9^{4-} species, including these species as neat sodium salts, has been obtained by the von Schnering group from synthetic, X-ray powder diffraction, and vibrational spectroscopic studies but without clear X-ray resolution of the two structure types due to poor crystal quality (twinning, high pseudosymmetry).[61] (The results from Sevov et al. generally pertain to larger cations.)

2.4. Mixed Element Clusters

There is little doubt that more isoelectronic and substantially isosteric cluster analogues of those in Table 3 will be prepared, and perhaps also some unimaginable species when mixtures of cations (see Section 4) or of p-metals from different groups are employed. A few examples of the latter were noted in Table 1, $TlSn_3^{5-}$ is another in Table 3, and more will be discussed in the next Section. But some attempts will give surprises, accessing different types of cluster structures that are not stable (or have not yet been achieved) under the homoatomic regime. Two early examples, using zinc or cadmium, are noted in Table 3: Attempts to increase the charges on tetrelide clusters, which depend only on the deltahedral type and not on cluster size, gave novel results instead, as condensed or interbridged oligomers in the diamagnetic Cs_6ZnGe_8 and metallic K_6CdPb_8 examples. The first, $ZnGe_8^{6-}$, can be viewed as two Ge_4 tetrahedra each face-bonded (μ_3) to a central zinc atom to give an effective D_{3h} symmetry, that is, two fused trigonal bipyramids, $Ge_4ZnGe_4^{6-}$. The second contains separate Pb_4^{4-} units and $Cd_3Pb_{16}^{10-}$ oligomers in a 2:1 ratio: The $Cd_3Pb_{16}^{10-}$ consists of pairs of $CdPb_8^{6-}$ units (analogous to $ZnGe_8^{6-}$) that are further interbridged by a six-coordinate Cd^{2+} again μ_3-bonded to faces of the end lead groups as $(Pb_4CdPb_4)Cd(Pb_4CdPb_4)^{10-}$. Other examples are the similar Cs_6HgPb_8 with a mercury atom bridge between edges of the two lead tetrahedra,[62] and $Tl_2Te_2^{2-}$, which is butterfly, not tetrahedron, shaped.[63] To date, these contrary geometries all occur with elements differing by two or more groups, but this alone is not a sufficient condition. Inclusion of gold in Tt_4^{4-} and related species generally gives condensation into infinite chains, for example $^1_\infty[Tl_4Au^{3-}]$,[64, 65] but will not be considered further.

3. Triel Clusters: Beyond the Zintl Boundary

An obvious condition to provide analogues for the electron-poorer trielides is that classical examples have one more negative charge per atom than the comparable tetrelides, that is, *closo*-$Tr_n^{(n+2)-}$ is equivalent to *closo*-Tt_n^{2-}. In addition, the foregoing Sections have anticipated one other change that is apparently necessary to prepare trielide clusters: sufficiently large Madelung energies in the compact solid state with only more-or-less small, closely packed naked cations. Thus, molecular solvents are (evidently) insufficient, with or without cryptand or equivalent, to separate the ions and yield solutions of the same polyanions. The alloylike structural results that led Zintl to exclude valence-compound prospects for the trielides beyond the Zintl boundary (Section 5), was at the time based on the structure types that these compounds formed with excess magnesium.[13] With 60 years of subsequent experience, we now know that magnesium is not the best "test" cation; in fact, there are only a few alkaline-earth systems for which there is any information relevant to this review. In any case, the Zintl boundary is now certainly a less general and useful delineation than originally considered for the formation of classical polyanions. For the moment, we will deal primarily with both the classical (Wade's rule) polyanions and, especially, those that fall short of these requirements and thereby expand our chemistry horizons into a new hypoelectronic cluster regime. Electron localization and relevant properties will be considered later with discussions of Zintl phases (Sections 5 and 6), although it is evident that with trielides we approach the land of intermetallic phases.[10, 66]

3.1. Classical Examples

The fact that the structure of Na_2Tl, which was (with my encouragement) investigated over 30 years ago, could be analogously formulated as $(Na^+)_8Tl_4^{8-}$ in terms of oxidation states[67] evidently gave the first hint that cluster results comparable to those for the then relatively unknown trielides might be achieved. Clearly, relatively small monovalent cations coupled with the larger, polyanionic atoms in the clusters are important for stability. As with A_4Tt_4 phases (A = Li – Cs), it was 25 years later that the smallest extension of the generality of trielide-cluster chemistry first appeared for the comparable Na_8In_4 as well as hypoelectronic examples.[68–71] At the other extreme, by the early 1980s the alkali-metal – gallium systems were becoming known for their numerous gallium – gallium bonded examples, but only in networks built entirely of what were new interbonded (or fused) gallium clusters and smaller gallium units, often very complex in detail.[72] At that time, the complex networks of electron-deficient gallium clusters were seemingly unrelated to Zintl phases of the later p-metals, although a couple of insightful articles relating the former to boron chemistry through Wade's rules had been published.[73, 74] (Analogous, discrete gallium clusters were not discovered until quite recently.) Notwithstanding, the connection between the cluster chemistry of gallium in networks and that of the heavier, later p-metals was not recognized until the cluster chemistry of the latter and the applicable electronic rules became clearer. In fact, the first investigations on alkali-metal systems of indium were undertaken with other objectives.

Classical examples of trielide clusters, largely discovered along the way to the more novel results, are listed in Table 4.

Table 4. Classical[a] anionic clusters of the triel elements (Tr) that are stable as neat salts.

Ion	Compound	Cluster symmetry[a]	Skeletal p-electrons	Reference
Tl_4^{8-}, In_4^{8-}	Na_2Tl, Na_2In	$\sim T_d$ (*nido*)	$2n+4$	[67, 68]
	$Na_{23}K_9Tl_{15.33}$	$\sim T_d$ (*nido*)	$2n+4$	[75]
Tl_5^{7-}	$Na_2K_{21}Tl_{19}$	D_{3h} (*closo*)	$2n+2$	[76]
	$Na_{23}K_9Tl_{15.33}$	D_{3h} (*closo*)	$2n+2$	[75]
	$Na_9K_{16}Tl_{18}Cd_3$	D_{3h} (*closo*)	$2n+2$	[77]
In_5^{9-}	La_3In_5	C_{4v} (*nido*)	$2n+2$	[78]
Ga_6^{8-}	$Ba_5Ga_6H_2$	$\sim O_h$ (*closo*)	$2n+2$	[79]
Tl_6^{8-}	$Na_{14}K_6Tl_{18}M$ (M = Mg, Zn, Cd, Hg)	T_h	$2n+2$	[80]

[a] Following Wade's rules or equivalent.

These all involve atomic charges that are greater than one, and are found only for the smaller clusters and cations with a higher charge density or under special packing situations. For instance, two examples of trigonal bipyramidal Tr_5^{7-}, the direct analogue of Pb_5^{2-}, were in effect trapped in complex structures along with nonclassical clusters, for example in $(Na^+)_2(K^+)_{21}(Tl_9^{9-})(Tl_5^{7-})_2$ and $(Na^+)_{23}(K^+)_9(Tl^{5-})_{1.33}(Tl_3^{7-})_{0.33}(Tl_4^{8-})_2(Tl_5^{7-})$.The productive utilization of mixed cations will be elaborated later. The examples of isolated octahedral Tr_6^{8-} units are probably encountered because of particularly favorable lattice packing and the higher charge densities of the cations. More octahedra are certain to be found if enough systems are investigated thoroughly. The octahedral Ga_6^{8-} in $Ba_5Ga_6H_2$ is rigorously D_{3d} (described as approximately O_h in Table 4). This cluster was first reported[81] for a composition that was difficult to understand, presumably that of a metallic phase $(Ba^{2+})_5(Ga_6^{8-})(e^-)_2$. However, experience has shown that closed-shell Zintl compounds predominate in this sort of chemistry, a condition that has been implicit in nearly all of the examples discussed heretofore and which will be considered later in more detail. Thus, the answer for the apparent inbalance here was found in hydride impurities, namely, reformulated to $Ba_5Ga_6H_2$ with hydride located in the better-sized pair of barium tetrahedra (see Figure 2). Hydrogen

Figure 2. The structure of $Ba_5Ga_6H_2$, with trigonal antiprismatic Ga_6^{8-} and hydride in barium tetrahedra.

contamination is now known to be a particularly insidious problem, even with the best alkaline-earth metals available commercially.[82, 83]

Finally, the formal In_5^{9-} ion in La_3In_5 is a forecast of probable things to come. In this case, the relatively few higher-charged cations appear insufficient to separate the classical square pyramidal (*nido*) indium clusters well, and some intercluster indium–indium distances remain that are only 11–15% (0.33–0.48 Å) greater than the average intracluster bond lengths. (These, in fact, are important in occupied band states.) The experimental result is a metallic compound. (A possible role of the high field La^{3+} has not been examined.) Of course, the metallicity is a property of the weakly bound electrons and the lattice, whereas the well-defined cluster shape is a reflection of more tightly bound valence electrons. Clearer examples of this isolated cluster type are certain to be found through the utilization of a greater number of cations with lower charges.

3.2. Hypoelectronic Trielide Clusters

Exploratory synthesis efforts within the alkali-metal–triel systems, for indium and thallium especially, have revealed many novel and unanticipated features about their chemistries, not just new classical species, structures, and stoichiometries, but also the presence of evidently the first hypoelectronic clusters relative to Wade's classical rules. For a long time, the minimum for skeletal electron counts in traditional main-group element clusters was taken to be the $2n+2$ electrons for *closo*-deltahedra, but this apparent boundary existed only because this "rule" had never been adequately tested. The trielides provide such a new chemistry not only in homoatomic naked clusters, especially Tr_{11}^{7-}, but also for centered polyhedra such as $ZnIn_{10}^{8-}$. Indeed, the unusual presence of centered (interstitial) atoms in some clusters is comparable to that requirement for many of the rather distant $M_6(Z)X_{12}$-type clusters of the early transition metals M (interstitial Z, halide X).[84]

Table 5 summarizes discrete hypoelectronic clusters as 1) homoatomic, 2) substituted, and 3) centered examples. The electronic classification of the last group depends to some extent on the point of view. (Other examples, found in networks such as icosahedral gallium, appear in Section 5.2.) The four new examples in the homoatomic category are shown in Figure 3. The Tl_6^{6-} (a) and Tl_7^{7-} (b) reflect conventional (Jahn–Teller) axial compressions of the conventional octahedron and the uncommon pentagonal bipyramid, respectively. These changes are methods to reduce the relatively large cluster charges on the normal polyhedra (-8 and -9, respectively). A transannular bond is achieved only in Tl_7^{7-}, 0.1–0.2 Å longer than in the remainder of the cluster, although the larger equitorial ring for this example already situates the axial atoms so close that the ideal $(2n+2)$ model may not apply. The distortion for each example drives the out-of-phase σ^* (a_2') combination of p_z orbitals on the axial atoms energetically higher and free of occupying electrons. It will be noted later that the structures of K_6Tl_6 and Cs_6Tl_6 are alternatives for the similarly four-bonded, stuffed-diamond structure of NaTl (Section 5.1) since the K^+ and Cs^+ ions are too large to fit comfortably within the (formal) Tl^- network. (The RbTl member does not exist.) The unprecedented Tl_9^{9-}

Table 5. Hypoelectronic clusters of triel elements.

Ion	Compound	Cluster symmetry[a]	Skeletal p-electrons[b]	Reference
Homoatomic				
Tl_6^{6-}	KTl	$\sim D_{2h}$	12 ($2n$)	[85]
	CsTl	$\sim D_{4h}$	12 ($2n$)	[86]
Tl_7^{7-}	$Na_{12}K_{38}Tl_{48}Au_2$	$\sim D_{5h}$ (C_{2v})	14 ($2n$)	[87]
	$K_{10}Tl_7$[c]	$\sim D_{5h}$ (C_{2v})	14 ($2n$)	[88]
Tl_9^{9-}	$Na_2K_{21}Tl_{19}$	C_{2v}	18 ($2n$)	[76]
	$Na_{12}K_{38}Tl_{48}Au_2$	C_{2v}	18 ($2n$)	[87]
Ga_{11}^{7-}	Cs_8Ga_{11},[d] $Cs_8Ga_{11}Cl$	$\sim D_{3h}$	18 ($2n-4$)	[89]
In_{11}^{7-}	K_8In_{11},[c] Rb_8In_{11}, Cs_8In_{11}	$\sim D_{3h}$ (D_3)	18 ($2n-4$)	[69–71]
Tl_{11}^{7-}	A_8Tl_{11}[c] (A = K–Cs)	$\sim D_{3h}$ (D_3)	18 ($2n-4$)	[90]
	$A_{15}Tl_{27}$[c] (A = Rb, Cs)	D_{3h}	18 ($2n-4$)	[91]
	$K_{18}Tl_{20}Au_3$[c]	D_{3h}	18 ($2n-4$)	[92]
Substituted				
$Tl_9Au_2^{9-}$	$K_{18}Tl_{20}Au_3$[c]	D_{3h}	16 ($2n-6$)	[92]
$Tl_8Cd_3^{10-}$	$Na_9K_{16}Tl_{18}Cd_3$[d]	D_{3h}	18 ($2n-4$)	[77]
$In_{10}Hg^{8-}$	$K_8In_{10}Hg$[e]	$\sim D_{3h}$	18 ($2n-4$)	[93]
Centered				
$In_{10}Zn^{8-}$	$K_8In_{10}Zn$	D_{4d}	18 ($2n$)	[94]
$Tl_{10}Zn^{8-}$	$K_8Tl_{10}Zn$	D_{4d}	18 ($2n$)	[95]
$Ga_{10}Ni^{10-}$	$Na_{10}Ga_{10}Ni$	$\approx C_{3v}$	20 ($2n$)	[96]
$In_{10}M^{10-}$	$K_{10}Tr_{10}M$ (M = Ni–Pt)	$\approx C_{3v}$	20 ($2n$)	[97]
$Tl_{10}M^{10-}$	$K_{10}Tr_{10}M$ (M = Ni–Pt)	$\approx C_{3v}$	20 ($2n$)	[98]
Tl_{13}^{10-}	$Na_4A_6Tl_{13}$[d] (A = K–Cs)	T_h	25 ($2n+1$)	[99]
Tl_{13}^{11-}	$Na_3K_8Tl_{13}$	D_{3d}	26 ($2n+2$)	[99]
$Tl_{12}Na^{13-}$, Tl_6H^{7-}	$Na_{15}K_6Tl_{18}H$	T_h	26, 14 ($2n+2$)	[100]
$Tl_{12}M^{12-}$, Tl_6^{8-}	$Na_{14}K_6Tl_{18}M$ (M = Mg, Zn–Hg)	T_h	26, 14 ($2n+2$)	[80]

[a] Neglecting heteroatoms. [b] Skeletal electron counts exclude ns^2 cores, while n values for polyhedra exclude the centered atom, if any. [c] Metallic phase; stoichiometric but not electron precise. [d] Curie–Weiss paramagnetic salt. [e] Hg is disordered over trigonal prismatic sites.

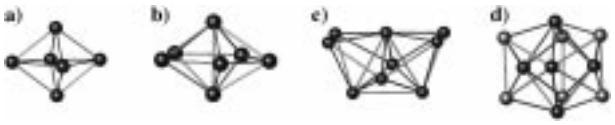

Figure 3. Four unusual trielide anions found in neat salts: a) tetragonally compressed Tl_6^{6-} in CsTl; b) Tl_7^{7-} in $K_{10}Tl_7$; c) Tl_9^{9-} in $Na_2K_{21}Tl_{19}$; d) Tl_{11}^{7-} from K_8Tl_{11}, with the atoms defining the trigonal prism drawn lighter.

cluster (Figure 3c) has now been captured in two different compounds (Table 5), as have Tl_5^{7-} and Tl_7^{7-} clusters. The derivation the configuration of Tl_9^{9-} from the common nine-atom polyhedral shapes (D_{3h} or C_{4v}) is fairly tortuous, but the result is readily achieved by removal of four adjoining atoms from the centered Tl_{13}^{11-} icosahedron (see below), which exposes the formerly centered thallium atom (at the top of Figure 3c). The Tl_7^{7-} cluster is also a fragment of the same parent.

The important entrée into new hypoelectronic clusters that are achieved through distortion, and the most common example among the trielides, is In_{11}^{7-} and its descendants, all of which are very close to D_{3h} symmetry. The anion in K_8Tl_{11} is shown in Figure 3d with the trigonal prism highlighted. With the clarity of hindsight, this polyhedron is readily achieved conceptually through first capping the basal faces of the (hypothetically *closo*) tricapped trigonal prism Tl_9^{11-} by two thallium cations, which introduces no new skeletal orbitals or electrons. The two new vertices are at this point rather exposed and of low order in bonding, but a logical axial compression and radial expansion both adds bonding between axial and equitorial capping atoms and empties the formerly bonding a_2'' orbital within the trigonal prism [Eq. 1]. The a_2'' orbital consists of p_z orbitals that are π bonding within the basal faces but antibonding along the prismatic edges, so that a loss of π bonding upon lateral expansion and increased antibonding effects upon compression make this orbital both energetically high and empty. (The opposite distortion stabilizes the D_{3h} form of the $2n+4$ electron polyhedron Bi_9^{5+}, see Section 2.2.) Hence, the combination of capping and distortion converts the former ($2n'+2$) Tl_9 polyhedron to the new and more symmetric ($2n-4$) Tl_{11} cluster with a lower charge ($n=n'+2$). The stability of the seven examples of binary A_8Tr_{11} compounds are logically dependent on the competing, alternative phases present in the various systems, that is, either A_8Tr_{11} or the A_2Tr_3 phase, but not both.[89] This accounts for at

$$\underset{2n+2}{Tl_9^{11-}} + 2Tl^+ \xrightarrow{\text{caps on } C_3} \underset{2n-2}{Tl_{11}^{9-}} \xrightarrow{\text{distortion}} \underset{2n-4}{Tl_{11}^{7-}} + 2e^- \quad (1)$$

least some of the surprise associated with the occurrence of the smallest cluster (Ga_{11}^{7-}) with the largest cation (cesium), but this product is irregular in other ways too.

The contrast between cation count (8+) and the closed-shell cluster charge (7−) in the A_8Tl_{11} phases defies, of course, the traditional belief that their magnitudes should match. Accordingly, the A_8Tl_{11} phases join a limited list of "metallic salts", of which TiO, CeS, and LaI_2 are simple members. The resistivities of A_8Tl_{11} phases are still moderate (a few hundred $\mu\Omega$cm), metallike in their temperature dependencies, and their magnetic susceptibilities are characteristic of Pauli paramagnetism (except for Cs_8Ga_{11}). The evident answer is that one extra cation per formula is necessary for good packing in the rhombohedral A_8Tr_{11} lattice; a [110] section for K_8Tl_{11} is shown in Figure 4. More examples of this particular behavior are found in other trielide systems (examples to follow). Two ways have been found to capture the extra electron in A_8Tr_{11} while retaining the basic crystal structure. Substitution of one indium atom by mercury (disordered over the trigonal prismatic sites) in K_8In_{11} yields the diamagnetic product $K_8In_{10}Hg$. Alternatively, a halogen (X = Cl–I) added to a variety of A_8Tr_{11} systems becomes bound in a distorted version of an A_8 cavity that was already present in the binary A_8Tr_{11} structure, and this change afforded nine diamagnetic $A_8Tr_{11}X$ phases. In three cases, these ternary halides exist in systems in which the binary

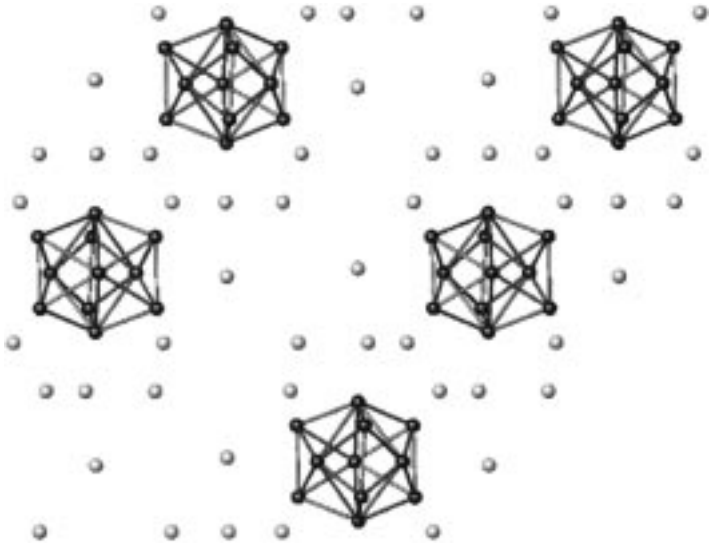

Figure 4. A [110] section of the rhombohedral structure of K_8Tl_{11}.[69]

phase is evidently not stable (Rb–Ga, Rb–In, Cs–In). We have not been able to reproduce a report of Rb_8In_{11}.[71]

Two other products of a substitution in the Tl_{11}^{7-} polyhedron have different characteristics and new features. Gold substitutes on the two axial (threefold-symmetric) sites, which would, without modification, give a $Tl_9Au_2^{9-}$ unit that is four electrons short. This is remedied by the addition of two electrons plus the formation of a strong transannular bond ($d_{Au-Au} = 2.96$ Å) between the former capping atoms (see Figure 5a). The remaining thallium framework changes very

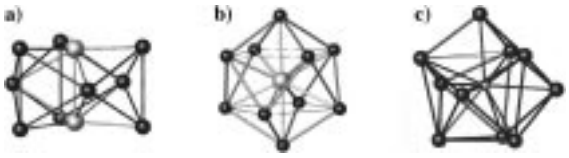

Figure 5. Centered clusters of the trielides: a) $Tl_9Au_2^{9-}$, b) $Tl_{10}Zn^{8-}$, c) $Ga_{10}Ni^{10-}$.

little in this process so the product is essentially a tricapped trigonal prism with centered basal faces. The independent unit in the structure, $(K^+)_{18}(Tl_9Au_2^{9-})(Tl_{11}^{7-})(Au^-)(e^-)$, contains both an isolated and essential Au^- ion and an extra, evidently delocalized, electron. The cation count seems quite certain. On the other hand, a more standard substitution, $Tl_8Cd_3^{10-}$ within $Na_9K_{16}Tl_{18}Cd_3$, puts the heteratoms in the waist-capping positions. This structure also contains a pair of Tl_5^{7-} anions *and* an extra electron per cell, $(Na^+)_9(K^+)_{16}(Tl_5^{7-})_2(Tl_8Cd_3^{10-})(e^-)$. However, the extra electron for both $Na_9K_{16}Tl_{18}Cd_3$ and Cs_8Ga_{11} does not produce a metallic property. Moreover, no significant change in the cluster dimensions or contact distances appears in either compound, suggesting that electrons are not trapped in antibonding (LUMO, etc.) cluster orbitals, at least on a single unit. The electrons are instead evidently (Mott-)localized, possibly held in some multication cavity, where they yield typical Curie–Weiss magnetic signatures (1.50 and 1.43 μ_B, respectively). These phases may be similar to Pr_2I_5 in this character.[101, 102]

3.3. Centered Trielide Clusters

Another pleasant surprise in polytrielide chemistry is the occurrence of a family of novel centered clusters. Two $Tr_{10}Zn^{8-}$ members (Tr = In, Tl) exhibit zinc addition to the center of a standard (D_{4d}) bicapped square (Archimedian) antiprism (Figure 5b), a process that also includes the effects of distortion. The parent cluster again undergoes a tetragonal compression and lateral expansion, presumably to achieve more nearly equivalent Tr–Zn distances, which likewise enlarges the two basal (square) planes and raises the corresponding bonding a_1 molecular orbital to a future LUMO role. Addition of a centered *neutral* zinc atom then causes the loss of one bonding a_1 orbital and two electrons (since both of the totally symmetric s-like orbitals were occupied), and an appreciable stabilization of the remaining orbital through mixing with the zinc 4s orbital (Scheme 1).

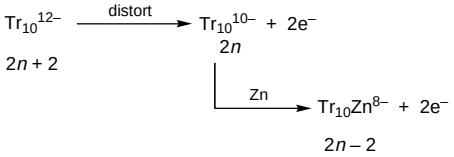

Scheme 1. The transition from the ideal Tr_{10}^{12-} cluster to the centered $Tr_{10}Zn^{8-}$ cluster.

Similarly, the 4p orbitals on zinc stabilize existing cluster states while three corresponding antibonding orbitals appear. An alternative view is to retain the electron pair in the weakly stable, distorted Tr_{10}^{12-} unit and to add Zn^{2+}, which stabilizes one and empties another a_1 level. The $2n-2$ electron-count result is in either case the result of the distortion.

The formation of the isoelectronic $Tr_{10}M^{10-}$ clusters (Tr = Ga, M = Ni; Tr = In, Tl, M = Ni, Pd, Pt) does not give the same geometric result, for reasons that may be rather unfamiliar in molecular chemistry but which appear important in compact ionic compounds in the solid state. The reduced $\sim C_{3v}$ symmetry of the $Tr_{10}M^{10-}$ polyhedron evidently manifests the presence of (or need for) strong interactions of the polyanion with the two additional cations (see below), and the polyhedron is opened to provide additional edges and faces of a roughly tetracapped trigonal prism. In Figure 5c the gallium member $Ga_{10}Ni^{10-}$ is shown with the uncapped basal face at the bottom. The bonding effects in $Ga_{10}Ni^{10-}$ and $In_{10}Ni^{10-}$ show some close parallels with those in the isoelectronic $In_{10}Zn^{8-}$, starting with the similar tetracapped $(2n)$ Tr_{10}^{10-}. The principal nickel bonding occurs via the 4s and 4p orbitals, particularly the former, while the nickel d^{10} manifold lies about 5 eV lower, corresponding to a well-reduced Ni^0 core. The average number of trielide neighbors and the Tr–Tr overlap population at each vertex are greater than in the zinc-centered cluster, as is the number of neighboring potassium cations that show rather specific interactions with the cluster at faces, edges and vertices (see

Section 4). Both the nickel- and zinc-centered compounds are diamagnetic. It is interesting to note that three types of 11-atom clusters all have 40 cluster-based electrons when ns^2 cores are included, $Tr_{10}Zn^{8-}$, $Tr_{10}Ni^{10-}$, and Tr_{11}^{7-}. The Tt_9^{4-} polyhedra are also 40-electron species.

The trielide explorations have also revealed a new family of naked polyhedra, the self-centered (*closo*) Tl_{13} icosahedra. Although these species are, for the most part, not hypoelectronic, they are included in Table 5 with other centered examples. Better precedents of fragments of this polyhedron are the uncentered borane $B_{12}H_{12}^{2-}$ and the network of icosahedra interbonded at vertices of α-boron. The nominal $6s^2$ cores on thallium can be viewed as alternates to the exo B–H or B–B bonding functions in the boron compounds. The delocalized bonds in the thallium polyhedra are longer and weaker than for boron, and the observation of only endohedral (centered) examples for such a large polyhedron seems reasonable. The added member can be either a 13th Tl atom, or a cation of a more active metal. (Empty Ga_{12} clusters are also known in cluster networks—see Section 5.2.) As will be detailed later in Section 4.2, the packing of cation neighbors about the approximate icosahedra seems to be of paramount importance.

Among the self-centered examples, the somewhat more versatile structures of the stoichiometric cubic $Na_4A_6Tl_{13}$ (A = K–Cs) contain the odd-electron Tl_{13}^{10-} cluster (Figure 6). Evidently, the particular environment with ten cations, especially the 8/2 Na^+ near neighbors (see below), is structurally more important than achievement of a closed-shell Tl_{13}^{11-} cluster (*closo*-Tl_{12}^{14-} plus a centered Tl^{3+}). The symmetry of the cluster is T_h and the space group $Im\bar{3}$. The unit cell is shown in Figure 7a. The radial distances within the anion are all equal and short, 3.225 Å, while those on the surface distribute between six smaller values, 3.281 Å for the edges bisected by three perpendicular twofold axes and 3.416 Å between these edges. The electron hole in these phases is evidently localized, as they exhibit Curie–Weiss paramagnetism with μ_{eff} values of (Rb) 1.74 and (Cs) 1.90 μ_B, and $g = 2.01$ for both. Provision of other interstitial elements yields an interesting family of mixed octahedral and icosahedral clusters in a related cubic structure (see below) that retain much of the strong and effective packing of $Na_4A_6Tl_{13}$.

Figure 6. The Tl_{13}^{10-} cluster in $Na_4K_6Tl_{13}$.

The closed-shell Tl_{13}^{11-} has so far been achieved only as the stoichiometric rhombohedral $Na_3K_8Tl_{13}$, with the cell illustrated in Figure 7b. The lower symmetry $R\bar{3}m$ space group gives a D_{3d} symmetric Tl_{13}^{11-} cluster with two slightly different radial distances and three distinct surface separations: 3.22 Å for those equivalent to the three *trans* bond pairs in Tl_{11}^{10-} and two longer ones, 3.42 and 3.58 Å. This phase has weak Pauli paramagnetism and is a modest metallic conductor, approximately 70 μΩ cm at 293 K, whereas the $Na_4A_6Tl_{13}$ compounds are poorer metals. These last two features, not uncommon among trielide phases, will be a subject of consideration in Section 6. The phase fields of the two stoichiometric Na-K-Tl cluster compounds $Na_4K_6Tl_{13}$ und $Na_3K_8Tl_{13}$ are well separated and distinct (compare ref. [103]). A novel variation for the former cubic structure $A_4(A')_6Tl_{13}$ has been reported in the phase $K_6(NaCd)_2(Tl_{12}Cd)$ by Belin and co-workers[104] (see also the end of Section 4.2). Insertion of Cd into the Tl_{12}^{14-} clusters alone would leave the system short four electrons per unit cell. In fact, the deficiencies are compensated by random

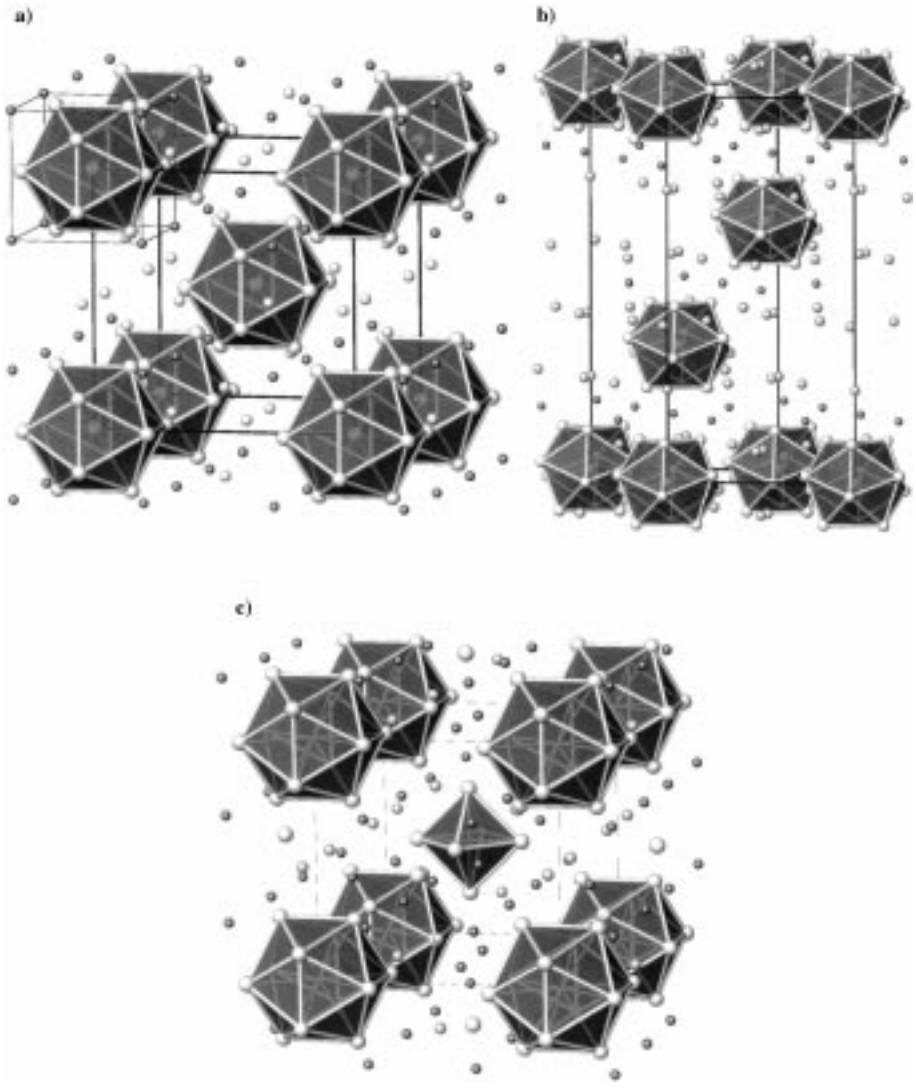

Figure 7. a) The centered cubic unit cell of $Na_4K_6Tl_{13}$, with sodium as the darker isolated atoms; b) the rhombohedral cell of $Na_3K_8Tl_{13}$; c) the primitive cubic cell of $Na_{14}K_6(Tl_{12}Na)(Tl_6H)$.

substitution of about 50% of the four Na^+ sites by Cd^{2+} ($Z = 2$). Support for this novel arrangement is strong, as determined by crystallographic refinement and also by direct analysis of single crystals from a synthesis at that stoichiometry. Although the refinement of cations of post-transition elements on alkali-metal sites has in general raised some concerns (because of the strongly reducing polyanions present), the supporting chemical analyses here and the fact that the product is properly a fairly poor semiconductor make this instance very logical. The cadmium cations, dispersed among an equal number of inner sodium sites (see Section 4.1), provide more communication between the "not-so-naked"[104] clusters.

The presence of a little adventitious hydrogen in such cluster systems has also given a novel result, as has happened many times before. Reaction of a 2 Na:1 K:3 Tl composition yielded a related mixed-cluster compound with a slightly smaller primitive ($Pm\bar{3}$) rather than the body-centered cubic unit cell of $Na_4A_6Tl_{13}$. The structure (see Figure 7c) has a thallium octahedron centering a simple cube of $Tl_{12}Na$ units and the heavy atom composition $Na_{15}K_6Tl_{18}$. The odd-electron stoichiometry seemed amiss since the compound was not Curie–Weiss paramagnetic, and so hydrogen in the form of Tl_6H^{7-} was immediately suspected (only 0.02 wt.% H is needed).[83] Standard experiments confirmed this; none of this product was encountered when the sealed tantalum reaction container was heated in high vacuum, but it was produced quantitatively on either purposeful addition of a small amounts of H_2 or the use of a sealed silica jacket (which dehydrates slowly on heating) around the reaction container. The presumed formulation is therefore $(Na^+)_{14}(K^+)_6(Tl_{12}Na^{13-})(Tl_6H^{7-})$. (Note that H^- alone in a cation-defined cavity would not be suitable.) The structure can be easily derived from the centered cell composed of $(Na_4K_6Tl_{13})_2$ (Figure 7a) by substitution of one-half of the potassium by sodium about the octahedron, Tl_6H for one Tl_{13}, and $Tl_{12}Na$ for the other Tl_{13} in the primitive cell. Furthermore, other interstitials may substitute in the icosahedral fragment to give an isotypic series that contains empty octahedra and icosahedra centered by a divalent metal, namely $(Na^+)_{14}(K^+)_6(Tl_{12}M^{12-})(Tl_6^{8-})$ (M = Mg, Zn, Cd, Hg, but not Ca, Ni, Eu, Yb). Competition experiments show that the examples with centered divalent cations and empty octahedra are more stable than those with centered sodium and hydrogen atoms.

A fanciful extension of the last cluster structure (Figure 7c) is suggested as it shares an isotypic relationship with Mg_2Zn_{11} and Na_2Cd_{11}, which would be formulated in similar terms as $(M_{14}M'_6)(M_{13})(M_6)$ (M = Zn, Cd; M′ = Mg, Na).[80] Clear distinctions between nominal cations and cluster anions are lost as zinc now bridges between the zinc polyhedra that replace the thallium clusters, and so much more homogeneous bonding interactions are present. Thus we have, in the same structure type, basically crossed over the Zintl phase boundary between anion-forming substances in saltlike lattices and alloylike compounds. Some of the similarity is only geometric, but there are certain to be interesting, related bonding features to be deduced in Mg_2Zn_{11} and diverse analogues.

4. Cation Effects

4.1. Cluster "Solvation"

Experience with the structures of a wide variety of the present compounds that are characteristically polar or ionic gives compelling indications of both the importance of electrostatic interactions between ions or charged groups and how structures appear to maximize these effects by filling the spaces efficiently. "Nature abhors a vacuum", in salts anyway.

Close inspection of the diverse neat structures described here reveals that remarkably specific and transferable alkali metal dispositions occur about each cluster anion. The "solvation" environment always consists of cations that, in order of increasing distance from the anion, 1) cap cluster faces, 2) bridge edges, 3) are positioned exo (outward) at vertices. Although these cluster anions must have significant polarizabilities and therefore some covalent interactions with the cations as well, the electrostatic portion presumably dominates. Clearly, the strongest interactions are found with the shorter-ranged face-capping cation sites, within the limits of cation–cation repulsions. I will emphasize the nearest shell or two of cations about the anions, for it is really these "solvated" cluster anions that define our structural building blocks. It should be noted that the cations commonly show specific interactions with two or more clusters, these bridges serving to keep them apart since the polyanions would presumably condense or interbridge directly were they to come in contact. The whole collection of neat cluster structures affords a wide variety of polyanions on which very regular alkali-metal cation positioning can be observed, thereby allowing significant generalizations. The regularities seem surprising, but perhaps earlier comparisons of what we call "solvation" by cations have lacked such a variety of large anions.

Previous tables reveal some specific cation trends. Trielide clusters of the same type must have greater negative charges than related tetrelide members, and it is noteworthy that all neat, classical (Wade's rule) trielide clusters with charges greater than -1 per atom occur with either sodium or higher charged cations (see Table 4). This is especially noteworthy with the high (formal) charges on tetrahedral Tr_4^{8-}, where the smaller radii of curvature allows better accommodation of a relatively larger number of cations (see below). On the other hand, larger cations may be sufficient for many hypoelectronic (or other) clusters, where charge-per-atom values are all less than or equal to unity (Table 5). Several "odd" phases may be provisionally attributed to these packing effects, especially for paramagnetic Tl_{13}^{10-} in $Na_4A_6Tl_{13}$ where there is no room for the 11th cation (Section 4.2), and in the metallic A_8Tr_{11} phases. A few other electrides are rather inexplicable but presumably related, including $(K^+)_{10}(Tl_7^{7-})(e^-)_3$ and $(K^+)_{18}(Tl_{11}^{7-})(Tl_9Au_2^{9-})(Au^-)(e^-)$. The latter is not obtained without gold, and extra gold does not trap the odd electron, so the presence of a suitable cavity for Au^- is probably the critical point. This and other possible electron trapping means, as by a halogen, have not been widely explored.

4.2. Mixed Cations: A Synthetic Means for Increasing Variety

It is demonstrably true that many more trielide clusters may be isolated in the presence of mixed cations, a new and valuable "synthetic laxative" to expand variety. The interactions in binary systems are self-limiting as all cations are the same. The anions isolated are selectively those for which good packing schemes for their simple "solvates" are possible. Table 6 lists a number of mixed cation phases with their cluster contents that have been so achieved in thallium and (less explored) indium systems, all examples containing at least sodium and potassium. In fact, all trielide clusters, excepting Tr_4^{8-}, Tl_6^{6-}, Tl_7^{7-}, and Tr_{11}^{8-} are presently known only in compounds containing mixed alkali-metal ions (or higher charged cation components). Extensions to alkaline-earth metals and lithium should further the variations, although for lithium X-ray diffraction limitations and even special polylithium bonding states[10] may be encountered. The corresponding effects in the thallium network structures have scarcely been explored, but mixed cations of various types have been reported to yield many new gallium and indium networks.[107, 108] In general, one can imagine that a large variety of potential clusters may be captured from the starting alloy "soup", and one or more clusters obtained are subject to the availability of a suitable cavity in a "good" structure. Along this line, neutron diffraction studies on a variety of binary alkali-metal–p-metal melts give clear evidence that polyanions are present in the liquid state. Related indicators are found in thermodynamic properties, resistivities, and the like as a function of composition. Diffraction spectra of K/Tl and Cs/Tl melts also reveal surprising prepeaks, indicating some degree of intercluster ordering as well.[109, 110]

Table 6. Mixed cation stabilization of new phases and new trielide clusters.[a]

Formula	Clusters
$Na_2K_{21}Tl_{19}$	Tl_5^{7-}, Tl_9^{9-}
$Na_3K_8Tl_{13}$	Tl_{13}^{11-}
$Na_4A_6Tl_{13}$ (A = K–Cs)	Tl_{13}^{10-}
$Na_9K_{16}Tl_{18}Cd_3$	$Tl_8Cd_3^{10-}$, Tl_5^{7-}
$Na_{12}K_{38}Tl_{48}Au_2$	Tl_7^{7-}, Tl_9^{9-}
$Na_{14}K_6Tl_{18}M$ (M = Mg, Zn, Cd, Hg)	Tl_6^{8-}, $Tl_{12}M^{12-}$
$Na_{15}K_6Tl_{18}H$	Tl_6H^{7-}, $Tl_{12}Na^{13-}$
$Na_{23}K_9Tl_{15.33}$	Tl_4^{8-}, Tl_5^{7-}, (Tl_3^{7-}/Tl^{5-})
$Na_{26}A_3In_{48}$ (A = K–Cs)	network of *closo*- and *arachno*-In_{12}[105]
$Na_{4.8}K_{18.2}In_{39}$	network of *closo*-In_{12} and open In_{15}[106]

[a] References to the first eight are in Tables 4 and 5.

The following will enumerate the largely unpublished evidence for the specificity and variability of cation environments around some clusters. Four examples are shown in Figure 8. The special face-capping positions sought out by sodium ions are most evident, while the competition of sodium with the larger potassium (rubidium, cesium) ions at other sites is less readily interpreted but must also have to do with cation proportions, space filling, cation–cation separations, and so forth. On the other hand, it appears that sodium cations alone are too efficient at intercluster bonding in the sense that all binary Na/In and Na/Tl phases, except the two high-field Na_8Tr_4 compounds, occur in network structures

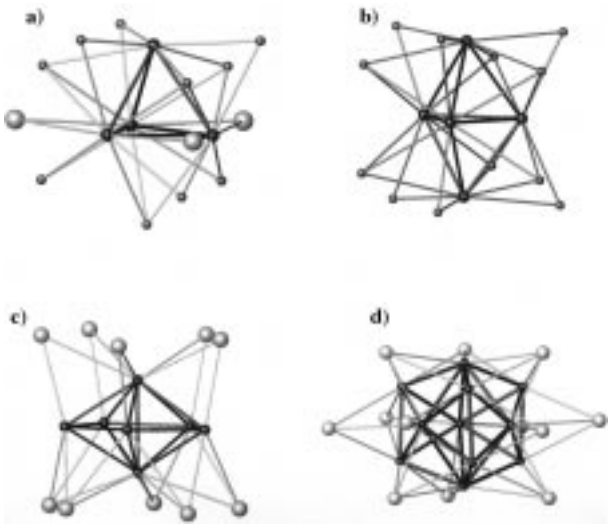

Figure 8. Cation environments about some cluster anions (black), with sodium as the smaller, lighter spheres: a) the $Na_{10}K_3Tl_4$ group in $Na_{23}K_9Tl_{15.33}$; b) $Na_{12}Tl_5$ in the same phase; c) the $K_{10}Tl_7^{3+}$ group in $K_{10}Tl_7$; d) the $K_{12}Tl_{11}$ clusters in K_8Tl_{11}.

in which Tr–Tr bonds usually interbridge between clusters, often in complex ways (see below). Some specific examples of cluster solvation follow.

Tr_4^{8-}: In the isostructural Na_2In and Na_2Tl, the nearest neighbor ions at increasing distances from the center of Tr_4^{8-} cap all faces, bridge all but one edge, and are exo at each vertex of each tetrahedron, such that the packing is a little irregular in this orthorhombic structure. In addition, all of the five independent types of sodium act as bridges between two or three clusters with some distribution of these functions.[68] The more symmetric Tl_4^{8-} component in $Na_{23}K_9Tl_{15.33}$ (see Figure 8a) has ten sodium atoms with a very similar motif on every face and edge, but with three potassium atoms bridging around one basal face and, further out, three more potassium atoms positioned exo at each vertex (not shown).

Tl_5^{7-}: In the same $Na_{23}K_9Tl_{15.33}$, the Tl_5^{7-} unit has all six faces and six edges bonded to sodium, but not the waist edges (see Figure 8b). Further out, there are also potassium atoms positioned exo at each thallium atom: three at each three-bonded apical thallium atom, and two at the less-negative, more-bonded thallium waist atoms (not shown). On the other hand, in the sodium-poorer $Na_9K_{16}(Tl_8Cd_3)(Tl_5)_2$, the sodium is face-capping and potassium is edge-bridging on one-half of each trigonal bipyramid, while the reversed roles appear for the other half. There are only exo potassium pairs around the waist. These dispositions are considerable more uniform than those around Tl_5^{7-} in the sodium-poor $Na_2K_{21}Tl_{19}$ where the essential sodium is only tetrahedrally bonded to a short edge on Tl_9^{9-} and to a long equatorial edge on the distorted Tl_5^{7-}.

Tl_7^{7-}: The cation neighbors and thence the presumed relative stabilities of these pentagonal bipyramids anions are distinctly different in $K_{10}Tl_7$ and $Na_{12}K_{38}Tl_{48}Au_2$, namely, $K_{10}Tl_7^{3+}$ versus $Na_4K_6Tl_7^{3+}$ in the first sphere. In the binary phase (see Figure 8c) potassium bridges edges on one pentagonal prism and caps faces on the other (this is in concert with out-of-plane waist bridging functions, not shown), while in the quaternary phase the cations alternate

face-capping roles in both halves of the prisms in the order K-Na-K-Na-K.

Tr_{11} $^{7-}$: Clusters in the family of rhombohedral A_8Tr_{11} (see Figure 8d, where the threefold axis is vertical) are surrounded by two independent types of cations. All six triangular faces about the waist (in pairs that share common prism edges) are capped by A2-type cations; each of these cations lies on a parallel threefold axis and thus has the same function in three adjoining clusters. Around each axial cap on the trigonal prism, three times as many A1-type cations (shown smaller in Figure 8) cap all the convex quadrilateral faces (bisected by the bond between capping atoms), bridge each edge of the trigonal pyramid, and are also exo at the three adjoining trigonal prismatic atoms. (The latter are omitted in the Figure 8d.) The same A1 cations also share these functions on adjoining clusters. An identical envelope of cations is found about the Tl_{11}^{7-} cluster in hexagonal $K_{18}Tl_{20}Au_3$.

$Tr_{10}Zn$ $^{8-}$: A single type of potassium atoms has three regular functions on this D_{4d} polyhedron (see Figure 5b), collectively capping the eight triangular faces around the waist of each cluster, bridging eight cap-to-antiprism edges in a second, and bonding exo to the eight thallium atoms in the antiprism of a third cluster. The apex atoms thus have bridges on the four adjoining edges but no cation positioned exo, the same relationship as in Tr_{11}^{8-} where these vertices also appear less accessible.

Tl_{13} $^{n-}$: The three cubic or rhombohedral structures of salts that contain centered icosahedra (see Figure 7) yield the clearest views of the "solvation" and of the roles of cations. Figure 9 shows the cation environments about Tl_{13}^{10-} and Tl_{13}^{11-} as they occur in space groups $I\bar{3}m$ and $R\bar{3}m$, respectively, with the clusters shown as shaded polyhedra. A very specific positioning of the cations on the icosahedra pertains to the whole series; every face (20) and vertex (12) is capped by a cation to give a fixed solvation sphere of 32 cations about each. Sodium atoms in specific positions are essential, and both their number and orientation define the structures. The eight face-capping sodium atoms (black) in $Na_4K_6Tl_{13}$ (Figure 9a) lie in a regular cube about the cluster (on the cell diagonals) with the other 24 potassium atoms defining a slightly distorted truncated octahedron. In $Na_3K_8Tl_{13}$ (Figure 9b), the sodium atoms define a trigonal antiprism (viewed here almost along the threefold axis). In both cases, the sodium cations are located in the center of chairlike puckered hexagons of potassium cations, and all are also shared with neighboring clusters. (Of course, no alkali metal bonding is implied by the connections drawn, which are only to guide the eye.)

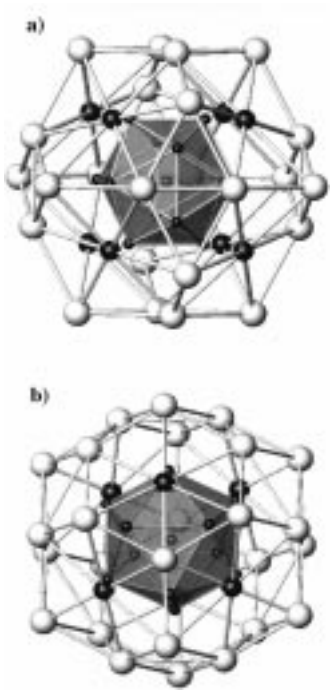

Figure 9. a) The Tl_{13}^{10-} cluster polyhedron in $Na_4K_6Tl_{13}$ with its neighboring eight sodium (small, black) and 24 potassium (larger, white) cations of its "solvation" sphere; b) the same representation of Tl_{13}^{11-} with Na_6K_{26} neighbors (D_{3d} symmetry).

In both structures, each sodium atom caps a triangular face on both the cluster shown and on a neighbor related by the particular symmetry: eight in the case of $Na_4A_6Tl_{13}$ and six in the case of rhombohedric $Na_3K_8Tl_{13}$. These Tl_3-Na-Tl_3 figures are trigonal antiprismatic and too small to accommodate any other alkali-metal cation. The loss of one of these cations from $Na_3K_8Tl_{13}$ puts more thallium atoms around each cation so that the cavities are larger in $Na_4A_6Tl_{13}$ and, it turns out, rubidium or cesium can be accommodated as well. But there is no room to pack an eleventh cation in $Na_4K_6Tl_{13}$, as the largest cavity remaining is tetrahedral with three cation vertices and a radius of 2.48 Å. Alternatively, the creation of an electron hole in the HOMO to give Tl_{13}^{10-} must simply cost energetically less than disruption of this well-packed structure. In other words, good packing in both structures requires two different sizes of alkali-metal cations in specific ratios, and so the phases appear to be stoichiometric and distinct. The prediction of alternate structural modes is very difficult, if not impossible, but from present evidence we conclude that good structures for any of the known Tr_{12} anions cannot be accomplished with cations of the same size.

Tl_6Z: The substitution of the body-centered cluster in $Na_4K_6Tl_{13}$ by a Tl_6 octahedron to give primitive cubic $(Na^+)_{14}(K^+)_6(Tl_{12}Na^{13-})(Tl_6H^{7-})$ (and equivalent), Figure 7c, is accompanied by substitution of six sodium for potassium neighbors around the smaller central cluster with a commensurate decrease in the lattice dimension of about 0.9 Å. Cation dispositions are otherwise very similar in both compounds. The all-sodium environment of the octahedron is shown in Figure 10. Among the three independent sodium atom types, the Na2 atoms still lie on the body diagonals of the cell and cap all faces on the octahedra and on 40% of the faces on the $Tl_{12}Na$ units that lie at the cell corners. Likewise, pairs of Na3 atoms are positioned exo to each octahedral vertex. The latter cations lie in pairs in pseudotetrahedral sites on each of the cell faces (e. g., at 0, ½, z; 0, ½, $\bar{z}$) where they bridge between Tl_6H^{7-} in adjoining cells

Figure 10. The Na^+ ions about Tl_6^{8-} in $Na_{15}K_6Tl_{18}$.

and positions on adjoining $Tl_{12}Na^{13-}$ units above and below. These two polyhedra and the space group have uniquely suitable symmetries for this arrangement. Of course, all of these features, especially the mixed cation precondition, apply to the extended family of isotypic $Na_{14}K_6(Tl_{12}M)(Tl_6)$ (M = Mg, Zn, Cd,…) where the now-empty octahedra are slightly expanded while the larger icosahedra are contracted on insertion of formally dipositive cations.

The special stability of the $Na_4K_6Tl_{13}$ packing (Figure 7a) is further emphasized by the discovery of the isostructural $(Na_2Cd_2)K_6Tl_{12}Cd$[104] noted before. Substitution of cadmium in Tl_{12}, as already known in the primitive cubic $Na_{14}K_6(Tl_{12}Cd)(Tl_6)$ (Section 3.3) and discussed in the previous paragraph, would by itself leave the cluster short by two electrons, but this is nicely compensated for by random replacement of half of the sodium by dicationic cadmium in the closest sites (Figure 9a). The phase is a semiconductor as the outer cadmium ions must serve to enhance the valence band width through intercluster interactions. Substitution of a tetravalent cation in the icosahedron instead, zirconium for instance, could give a diamagnetic product as well.

4.3. A "Good" Structure

There are many features that need to be considered to judge a "good" structure, and some of these judgements derive from subjective experience. A useful pedagogical example is shown in Figure 11, but it is not in any way a special one. The phase $Na_{12}K_{38}Tl_{48}Au_2$ occurs in space group $P\bar{6}m2$, with $(Na^+)_{12}(K^+)_{38}(Tl_7^{7-})_3(Tl_9^{9-})_3(Au^-)_2$ as the independent unit (again in terms of oxidation states), there being one such unit in the cell. The phase is stable over a sizable region of the quaternary system and with apparently fixed proportions of the four components, so there is something special about these ions, their sizes, and their packing in this structure. The clusters (black atoms) lie on unit cell faces and exhibit only mirror symmetry together with twofold axes at the plane intersections (*mm*2 or C_{2v}). The potassium and sodium positions are represented by the larger and smaller open spheres. Only the gold atoms (small solid spheres) lie on special points $\bar{6}$ at ⅓, ⅔, 0, and so forth. Little more can be judged from the illustration alone, and inclusion of bond representations between cations and clusters would make it quite inscrutable.

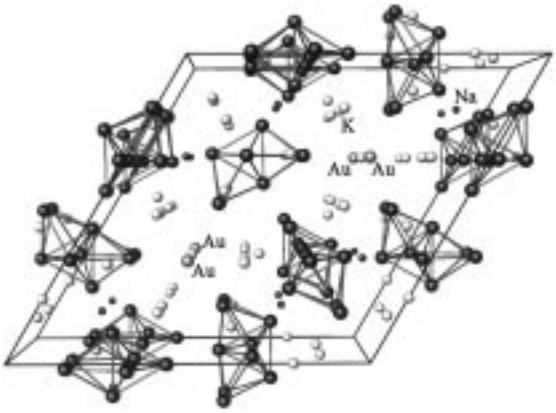

Figure 11. The $Na_{12}K_{38}Tl_{48}Au_2$ unit cell and its surroundings, with the Tl_9^{9-} and Tl_7^{7-} clusters emphasized. The alkali-metal and gold atoms are represented by small open and medium-sized black spheres, respectively. (This Figure is reproduced as the Frontispiece.)

Closer inspection of distances and local environments is necessary to assess the system well. In a general sense, all contacts between component ions seem reasonable. All cations bridge between clusters, sodium being especially effective at this bridging between faces on pairs of each type of cluster. These sodium connections are in fact chainlike because of the *mm* symmetry of the clusters. There are four to eight thallium atoms at typical distances about each cation (at somewhat greater distances for potassium), and six to eight cations about each thallium atom except at the less-exposed, face-centered atom on Tl_9^{9-} (i.e., the centered atom in the parent Tl_{13}; see Figure 3c). The shortest Tl–K, Tl–Na, and K–K distances are found around the apices in Tl_7^{7-}. Sodium atoms contact most thallium atoms in the structure by bridging four edges on the base of Tl_9^{9-} and capping four faces on Tl_7^{7-}. The 3.50 Å K–Au distances within the trigonal antiprismatic K_6Au are comparable to those in other cluster phases containing isolated gold and consistent with the eightfold 3.69 Å interatomic distance in CsAu (CsCl structure). The role of the two gold anions is evidently both to capture two extra electrons in the independent unit and to reduce repulsions within the cation lattice that lies between the clusters. The compound does not form without gold, nor will it take up more gold even though another free K_6 cavity of diameter 3.30 Å exists, presumably because of the lack of another electron. Other candidates to substitute for the gold anion, such as the larger halides, have not been tested.

Both clusters in this case are hypoelectronic ($2n$). It is, of course, necessary that the two clusters and Au^- have electronic structures and valence gaps that are consistent with a common Fermi energy. Further, the requirement of a periodic, three-dimensional structure must also be added to the "good" efficient packing and bonding implied above, all of which makes the overall result even more remarkable. Furthermore, the valence or oxidation state balance exhibited by this phase as well as by a large number of other cluster compounds is impressive and much more frequent than the formation of electrides or truly metallic phases with extra electrons.

5. Network Compounds as Zintl Phases

A further development of the concept of Zintl phases is now necessary beyond that given at the beginning of the review (Section 1). Many network compounds are also found to be valence compounds, even when electron-deficient clusters are involved, CaB_6 being a classic example. These are also collectively and usefully named Zintl phases. This descriptor is generally applied to compounds of active metals with p-metals that appear to have an electronically closed shell in their bonding, a condition that is often deduced from the structure alone.[111] Originally, Zintl applied this idea to

the maximally reduced monoanions of the main-group elements, and its applicability was later extended to more complex compounds in which the bonding could still be described by octet rules and which might be isostructural and isoelectronic with a following element (Si_4^{4-}, layered As, and so forth).[7, 8] More modern concepts have been incorporated regarding delocalized or electron-deficient bonding in networks, clusters, and so forth.[10] All of the neat cluster compounds already considered are in the general sense Zintl phases, save for the few odd examples. However, in this section we are concerned only with those phases exhibiting infinite bonding in one, two, or three dimensions. Some very complex examples are known, especially in gallium systems[108] and in mixed trielide–tetrelide or other p-metal combinations.[109] We will limit our considerations to a few network tetrelide and trielide examples that fit with the preceding material.

Clearly the Madelung part of phase stability must be very important here too, and the surface structures of the cations on the anionic networks as well (Section 4). These aspects are more complex in networks and have not been well explored or generalized. The problems of filling space in an efficient way in a three-dimensionally bonded network are more complex than with isolated clusters, and valence closure in some instances may be only approximately achieved. Clearly however, the considerable complexity of many structures reflects a drive to conform to some sort of valence rules.

Many tetrelide networks are achieved in combinations with electron-richer pentels (pnictogens), chalcogens, or the like, but these represent more of classical Zintl phase chemistry[8, 9, 109] which is not the intent of this article. Addition of cations to the tetrel elements classically gives structures related to those of later elements, for example, $CaSi_2$ that contains infinite sheets of 3b-Si^- with the arseniclike structure separated by cations.[7]. (In a shorthand often attributed to von Schnering,[122] 4b-Tr^- or 4b-Tt is conveniently used, where 4b means four-bonded Tr^- or Tt.) Packing differences in $SrSi_2$ and LiGe yield analogous 3b-Tt^- lattices with a defect diamond structure and cations in the interstices therein, while those in zig-zag chains of many 2b-Tt^{2-} are found in 1:1 alkaline earth metal salts with the CrB structure.

5.1. Tetrelide Networks

Some more novel tetrelide networks have been realized recently that exhibit different means of cation accommodation. One is the well-known clathrate-I structure $[A_{\leq 8}(H_2O)_{46}]$ that was originally assigned to the evident compositions A_8Tt_{46}. This presented problems, since the network of four-bonded tetrelide elements with cations in characteristic cavities apparently has no need or use for the electrons added by the eight alkali-metal atoms. The actual compounds in fact satisfy simple valence rules by incorporation of two specific tetrelide site vacancies (□), which in turn are each accompanied by four neighboring Tt^- sites that absorb the eight electrons from the cations, more explicitly, as $(A^+)_8$(4b-$Tt^0)_{36}$(3b-$Tt^-)_8\square_2$.[112, 113] Numerous isoelectronic, defect-free, and fully four-bonded variations of this have been generated by substitution of eight trielide atoms in the network, namely, $A_8Tr_8Tt_{38}$ (A = K–Cs; Tr = Al–In; Tt = Ge, Sn)[114] and with a change in cation as well, $A^{II}{}_8Tr_{16}Tt_{30}$ (A^{II} = Sr, Ba; Tr = Al, Ga; Tt = Si–Sn).[115] A different proportion of elements from the two groups and another expression of cation accommodation in a four-bonded helical net occurs in $Na(GaSn_2)$ which is more clearly described as $^3_\infty$[4b-Ga^-(4b-$Sn^0)_2$], Figure 12.[116] A very similar result with a different space group is found for $NaInSn_2$.[117] Anionic tin is particularly well known for its apparent drive and versatility to form closed-shell anions or networks in valence compounds, as examples witness the mixture of tin monomer and oligomer anions present in $Ca_{31}Sn_{20}$ [$\hat{=}$ $(Ca^{2+})_{31}(Sn^{4-})_5(Sn_2^{6-})_5(Sn_5^{12-})$], where all of the tin atoms have simple octet counts.[118] Likewise, the complex network in Na_5Sn_{13} has precisely five 3b-Sn^- per formula unit as expected.[119] Different variations are found in formal 3b-Tt^- products. A good number of other binary alkali-metal–tetrelide compounds evidently exist judging from phase diagrams,[120] but their correct compositions and structures are unknown and basically unimaginable.

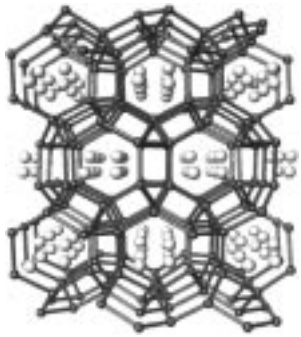

Figure 12. The structure of $NaGaSn_2$ with sodium ions (lighter spheres) ordered in zig-zag helical chains of $^3_\infty$[$GaSn_2$]. The Ga and Sn atoms are disordered.

5.2. Trielide Networks

Intrinsic to the trielides are greater degrees of interbonding and condensation and, in many cases, incorporation of electron-deficient clusters, but this trend may also be reversed to some degree by the addition of more cations. Nothing gives us the insights needed to predict these often complex structures.

There are many ways in which one can design an anionic four-bonded trielide framework. The most famous is that which is isosteric with cubic-packed diamond and with the elements silicon and gray tin, namely *the* Zintl phase NaTl,[121] shown in Figure 13. The structural problem that remains has to do with cation accommodation. In the case of NaTl, along with NaIn and LiTr (Tr = Al–In), the appropriate "stuffed diamond" NaTl-type structure is exhibited since these cations fit well enough in the alternate tetrahedral sites of the parent lattice. Detailed theoretical and property studies also support the original concept of a substantial charge transfer and directed Tl–Tl bonding.[123] On the other hand, this arrangement is ordinarily not possible for KTl and CsTl, presumably due to the size of the cation, and these exist instead as an $(A^+)_6Tl_6^{6-}$ cluster (see Table 5).

A different variation occurs in the layered structure exhibited by Cs_2In_3, Rb_2In_3,[124] and K_2Ga_3,[96] which have a straightforward electronic configuration. That for K_2Ga_3 is shown in Figure 14. The simple construction starts with an ideal Ga_6^{8-} octahedron, with 14 skeletal electrons ($2n+2$) in cluster molecular orbitals above six nominal $4s^2$ core states.

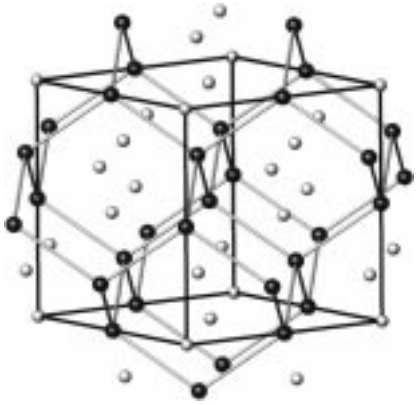

Figure 13. The cubic unit cell of NaTl emphasizing the Tl^- (diamond) net.

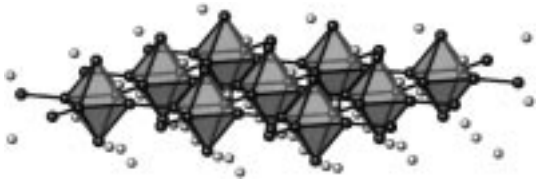

Figure 14. A portion of the layer of interbonded octahedra in K_2Ga_3.

Reduction of the cluster charge and layer generation can be imagined to arise by one-electron oxidation of each of the four $4s^2$ pairs about the waist of the octahedron to give the imaginary tetraradical ion $Ga_6^{\cdot\cdot 4-}$. Condensation of these in a planar array then yields the structure shown, the two-electron – two-center intercluster linkages being characteristically shorter than the electron-deficient Ga–Ga "bonds" (edges) within the clusters. Thus K_2Ga_3 is reduced $1\,e^-\,mol^{-1}$ from the three-dimensional interbridged network found in CaB_6.

Both versions of known, isolated trielide clusters (see Table 5) as well as new types are found in compounds with network structures. The gallium systems are particularly productive.[72, 107] Among the more striking are empty *closo*-Ga_{12} analogues of the $Tl_{12}M$ examples already described. A clear result occurs for Li_2Ga_7,[125] in which *empty* 12b-Ga_{12}^{2-} clusters are connected directly and through Ga_2^{2-} links, as shown in Figure 15a. The former are also found in K_3Ga_{13}.[126] Figure 15b shows how a new and smaller cluster variety, *closo*-Ga_8^{2-} dodecahedra, are bound into sheets and these sheets in turn bridged by isolated gallium atoms in AGa_3 (A = K – Cs).[127] Another novel phase, $Na_{10}Ga_6Sn_3$, contains Ga_{12} icosahedra bonded exo to terminal and bridging tin atoms to give chains.[128] A conventional formulation of this network would leave the structure short one electron per formula unit. A high yield synthesis to confirm the stoichiometry of the crystallographic analysis, particularly for sodium, was not possible. A second phase in this system, $Na_3Ga_6Sn_3$, contains layers of similarly interconnected Ga_{12} icosahedra interbonded to disordered Ga_2Sn_3 puckered layers. This is a valence phase according to the X-ray crystallography.[129] Empty, interbridged In_{12} clusters, together with other species, are found in $A_3Na_{26}In_{48}$[105] and $K_{18.2}Na_{4.8}In_{39}$,[106] among others.

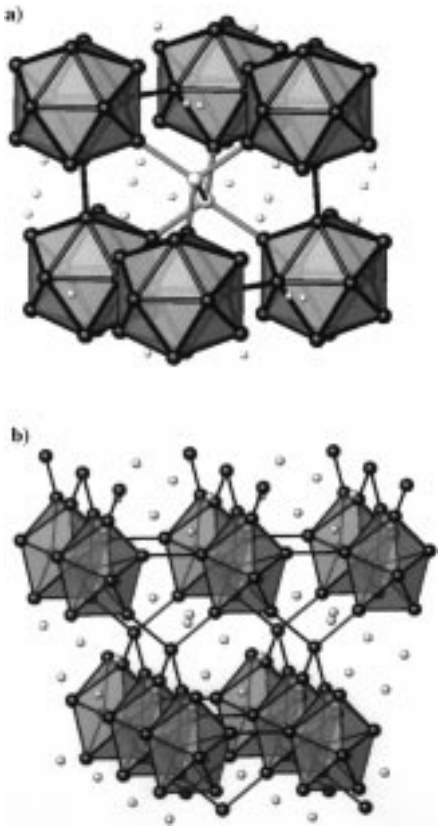

Figure 15. a) A portion of the structure of Li_2Ga_7 with isolated dimeric 6b-Ga_2^{2-} units interlinking sheets of interbridged Ga_{12} icosahedra. b) The tetragonal structure of KGa_3 with chains of interconnected triangular-faced dodecahedra linked by 4b-Ga^- atoms.

Other types of rather complex situations have been described and discussed,[72, 108, 109] while $K_{34}Zn_{20}In_{85}$[130] and $Na_8K_{23}Cd_{12}In_{48}$[131] are more recent examples.

Another condensed product shown in Figure 16, $Na_7In_{11.76}$,[132] affords useful lessons about new clusters, bonding, and a close approach to a valence compound in a fairly complex arrangement. Here, *nido* clusters derived from icosahedra ($\sim C_{5v}$ In_{11}) are seen to be linked apex-to-apex as well as each vertex exo bonded through a single bridging atom to ten other clusters, meaning the nominal isolated *nido*-In_{11}^{15-} $(2n+4)$ cluster has become In_{11}^{5-}. (The fractional stoichiometry comes about because of ⅜ vacancies at the apices of these clusters.) The other unit in this structure is a new polyhedron, an elongated (sodium-centered) *closo*-In_{16} cluster, that requires $2n+4$ skeletal electrons in isolation according to EHMO calculations. These polyhedra are oxidized too through intercluster bond formation at eight vertices, in part via triangular normal valent (3b-In^{2-}) linkages. Finally, MO calculations indicate that intercluster repulsion occurs between certain pairs of nonbonding electron pairs at exo positions on adjoining clusters. The total electron count, calculated to be necessary in consideration of all of these factors and complexities, comes to 99.4% of available electrons according to the refined composition; a remarkable closure that is probably within experimental uncertainties. The drive for closed-shell bonding is evident.

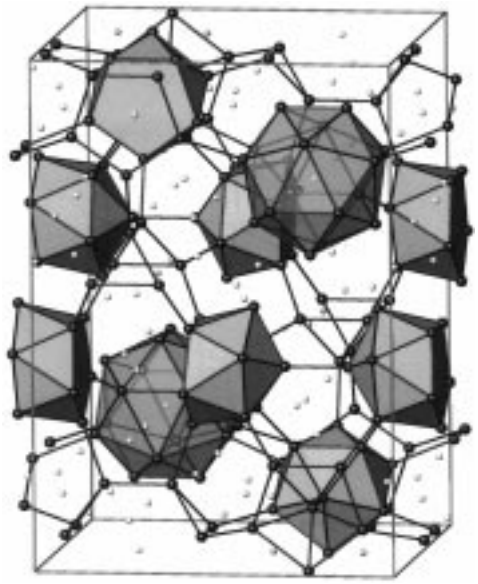

Figure 16. The tetragonal unit cell and surrounding atoms in $Na_7In_{11.76}$. Note the interbonded *closo*-In_{16} clusters, *nido*-In_{11} cluster dimers, and In_3 units.

One of the more novel results with thallium to date may be the columnar structure discovered for the composition $Cs_5Tl_{11}Cd_2$,[133] a piece of which is shown in Figure 17. This is generated from face-sharing, cadmium-centered pentagonal Tl_{10} antiprisms (equivalently, condensed cadmium-centered

Figure 17. A portion of the infinite augmented chains of condensed cadmium-centered Tl_{10} antiprisms in $Cs_5Tl_{11}Cd_2$.

and -capped thallium icosahedra) to which four-bonded thallium "fins" are added on one side. The lopsided rods pack into an hexagonal array, well separated by cesium cations. This phase appears to be a zero-gap semiconductor according to Hückel band theory calculations.

Finally, the "granddaddy" of all trielide cluster condensation products to date must be that found in a couple of complex indium "fulleranes". The In_{74} building block and the penultimate sodium sphere in the simpler $Na_{96}In_{97}Z_2$ (Z = Ni, Pd, Pt)[134] are shown in Figure 18. This actually is the outer part of a multiply endohedral unit constituted as $Ni@In_{10}@Na_{39}@In_{74}$. Note that the innermost $In_{10}Ni^{10-}$ unit (not shown because of some disorder) had already been recognized in the form of an isolated cluster (see Table 5), while the outer In_{74} cage has the same conformation as the regular fullerene C_{74} (but not its π-bonding). Not surprising, in light of the cation effects noted earlier (Section 4.1), is the duality exhibited by the intervening Na_{39} complement (represented as open spheres) which places a sodium cation on the inside of every face of the In_{74} unit. (A second, similar shell also occurs on the

Figure 18. The fulleranelike In_{74} cluster and the endohedral Na_{39} sphere (white spheres) of $Na_{96}In_{97}Ni_2$. The $In_{10}Ni$ core is not shown.

outside of every face.) The complicated part, which will not be detailed here, is the way in which this "stuffed buckyball" is incorporated into a three-dimensional solid. Every surface indium atom gains a fourth neighbor and an electron octet, either by condensation of the In_{74} units into close-packed layers through sharing of the six pentagonal faces around the waist of each unit or through some added In_3 and In_6 decorations bonded near the poles. Additional cations fall between the layers, some defining related $Ni@In_{10}@Na_{32}@In_{48}$-$Na_{12}$ units. The relationship between this complex $Na_{96}In_{97}Z_2$ (Z = Ni, Pd, Pt) and C_{74} are the same as between NaIn (stuffed diamond) and diamond. Furthermore, it differs from the NaIn composition only minutely, largely through the incorporation of a very few nickel, palladium, or platinum core atoms.

A second more complex phase, $Na_{172}In_{192}Z_2$,[135] exhibits many of the same general features. Two macroclusters, $Ni@In_{10}@Na_{37}@In_{70}$ and $Na@In_{16}@Na_{39}In_2@In_{76}$, are co-condensed into puckered layers as before. All faces on both "fulleranes" are capped on the inside and the outside by sodium atoms except for two indium atoms in the penultimate sphere within the second unit. These are bonded near an open site on In_{76} and serve as tethers by which the innermost $In_{16}(Na)$ cage unit is suspended! Isn't chemistry grand!

6. Properties and Philosophy

Implicit in the closed-shell assumption for the assignment of Zintl phases is that these compounds should be diamagnetic semiconductors, although this characteristic has generally been investigated only rarely. As considered before in more detail,[16] the properties of many of the trielide cluster phases are not so simple but, for some views, this does not always turn out to be of overwhelming importance as far as understanding the chemistry. One major value of the Zintl concept is in testing whether a new compound, its structure, and the electron distribution suggested therefrom are reasonable, whether important features such as impurities are perhaps missing, if something new in bonding is represented, or whether the compound is apparently metallic. Even the last feature is not necessarily fatal to our simple attempts to classify and understand cluster bonding.

A modest survey regarding electrical resistivities, magnetic susceptibilities, or both, of some of these tetrelide and trielide phases[16] reveals that only a few have resistivities with

appropriately negative temperature coefficients (e.g., Rb_2In_3, K_8Sn_{44}) while most have resistivities in the range of 200–800 μΩ cm with positive temperature coefficients. A larger number of phases are, nonetheless, diamagnetic (as opposed to Pauli-like paramagnetic) even after correction for orbital (Langevin) terms, including Na_2Tr, KTl, CsTl, $Na_2K_{21}Tl_{19}$, $K_{10}In_{10}Ni$, $K_8Tr_{10}Zn$, and $Na_{96}In_{97}Ni_2$. On the other hand, a good number of other examples that seem understandable in term of their structures are in fact Pauli-paramagnetic, for instance $Na_{23}K_9Tl_{15.33}$, $Na_{14}K_6Tl_{18}Mg$, and $Na_{12}K_{38}Tl_{48}Au_2$. Thus, $Na_3K_8Tl_{13}$ has a positive, approximately temperature-independent paramagnetism (circa 20×10^{-4} emu mol^{-1}) and a resistivity of only about 70 μΩ cm, suggesting it is a poor metal. In no case has any of these phases been characterized well enough to identify, or exclude, a semimetallic (indirect gap) property, a circumstance that would not in the simplest sense contradict Zintl concepts. In making conclusions on the basis of magnetic data, one should remember that many of the metals in this region are themselves diamagnetic because of nontraditional orbital and band properties.[2]

It is worth noting that essentially all of the phases under consideration here retain other characteristics long attributed to Zintl phases, especially saltlike brittleness, stoichiometric (line) formulations, and melting points above those of the component metals, whereas the magnetic properties suggest an approach to the intermetallic world is also in process.[3, 10, 66] Nonetheless, important considerations for our chemical understanding are that what we "see" in a structure can be predictably determined by the most tightly bound valence electrons (above ns^2 cores where appropriate), whereas the moderate resistive and Pauli-magnetic properties often found derive from a very small number of the most weakly bound electrons near the Fermi energy, for instance when band dispersion has closed the gap in a near-semiconductor. There is substantial evidence that the former matters more in these considerations; for example, we may usefully classify A_8Tr_{11}, $K_{18}Tl_{20}Au_3$, and so forth with "extra" electrons as "metallic Zintl phases" in which the bonding requirements associated with the clusters seem clear. In a different sense, La_3In_5 (Section 3.1) is a metallic Zintl phase apparently with a closed-shell cluster count but also inadequate intercluster separations. In fact, the square-pyramid clusters persist when the system is made electron richer in the isotypic La_3TrTt_4 and La_3Tt_5 analogues, the internal dimensions of the clusters changing only modestly and as expected from interactions of the LUMO cluster orbitals with the conductance band.[136] Note that these metallic cluster systems do not react in what some may consider to be an obvious way, in which the metal–metal bonds open upon reduction; rather, many bonded features frequently persist into the intermetallic region.

Nesper has aptly likened these situations to examining a submerged continent observed through an ocean of the conduction electrons, where it is the structure of the former that matters more.[10] Similarly, metallicity may come about when the nominally highest energy electrons or anions are instead delocalized, such as those in the highly reduced formal Tr^{5-} isolated atoms in both Y_5Ga_3 (Mn_5Si_3-type) and La_3InC (inverse perovskite),[16] and the hypoelectronic Ca_3Ga_5[137, 138] and Sr_3In_5.[139] A similar result appears to pertain to the π* electrons on the dimers in some Cr_5B_3-type compounds, which otherwise could be simply (or naively) formulated with closed-shell units as in $(Ca^{2+})_5(Sn_2^{6-})Sn^{4-}$. In fact these appear to be closer to multiply bonded dimers after π* electron delocalization.[140]

7. Trends and Forecasts

Some clear trends are evident in the foregoing, somewhat evolutionary, presentation. In the overall view, it is generally recognized that the transition from boron to thallium involves major changes in the chemistry, especially from strong and more directed bonds to more diffuse orbitals, more metallike behavior, and longer, weaker bonds. Considerable structural complexities in their compounds with the electropositive metals appear to be a common thread. The first step, an aluminum versus gallium comparison, has been largely ignored for metal-rich systems because there is so little that is comparable. Major differences in their fundamental properties are frequently cited as responsible (ionization energies, ionic and metallic radii, electronegativities, formation enthalpies, etc.) and attributed to the irregular intrusion of the 3d transition elements just before gallium with a resulting decrease in shielding of its valence electrons.[141] These sizable contrasts between properties of elemental aluminum and gallium do not reveal what the corresponding differences in their chemistry will be.[3, 66] Aluminum is certainly "harder" chemically and less electronegative, aluminides are generally more refractory, and their compounds with other metals are usually classified as intermetallics. At the same time, aluminides are still near the Zintl border in character and clearly exhibit significant homoatomic bonding, which usually maximizes bonding (overlap-weighted bond populations) within the aluminum framework but does not come near a closed bonding system (gap) electronically. For example, the complex two-dimensional aluminum framework found in $Ca_{13}Al_{14}$[142] certainly demonstrates that directional Al–Al bonding is still very effective and important and that manifestations of the Zintl-Klemm concept, especially strong homoatomic bonding, vanish slowly.[66, 143]

Gallium cluster chemistry has scarcely been described herein because, with few exceptions, so much of it pertains to complex networks, largely unrelated to the behavior of the rest of the family.[72, 108] In the words of the principal author Belin, "atom defections, atom substitutions, disorder, or nonstoichiometry often obscure the understanding of electronic and bonding requirements [in these networks]".[144] The theoretical basis for the fused clusters sometimes encountered is even more problematical.[145] The transition from gallium to thallium clearly involves considerable enhancement of the stability of isolated clusters, but not to an exclusive degree. Some largely unrelated network structures still appear for indium and thallium (to the extent that the explorations have been comparable for each element), but cluster anions of considerable variety dominate. Some important trends appear to operate in concert in the Ga →Tl transition—the apparent increase in the relative stability of the ns^2 pair down this series and a parallel decrease expected for the strengths of Tr–Tr

bonds (the enthalpies of formation of Tr(g) decrease by 36%). Since the imagined process for the formation of networks from clusters is oxidation of the ns^2 pair at each vertex (or some hybridized equivalent) followed by the generation of normal two-electon–two-center intercluster bonds, the expected trends for each step favor the formation of networks for gallium but clusters of thallium.

A pertinent question is often asked: why are the *anionic* states of the earlier p-metals so stable? To our knowledge this property has never been predicted or this strong proclivity well explained beyond the general electron deficiency of these elements and their compounds. One useful, but pretty simple, comparison is with energetic trends relative to the solid elements, that is, the relative energetics of disproportionation of these compounds into the component alkali and trielide metals when all changes in bond energies in the former are neglected. Since the gaseous states of both the sodium and gallium families are noteworthy for their relatively low enthalpies of condensation, there is simply less to be gained on decomposition of these compounds, or less to be required in countervailing bond strengths within the clusters.

Where next? So much of the excitement in exploratory synthesis is the discovery of the unpredictable and unimagined. On the other hand, some simple expectations come from just looking at the periodic table and the literature. Even a cursory look at the structures of the alkali-metal compounds formed by zinc and cadmium reveals numerous examples that can be interpreted as heavily condensed versions of clusterlike structures of the types seen here, a result that is appropriate to the lower electron populations. There must be a intermediate chemistry between these metals and the trielides. In addition, aluminum chemistry roughly along the lines of what has been seen for gallium family elements is too easy an expectation, and it will in fact be different in major and unimagined ways, as is already quite evident.

This article emphasizes the concept that a remarkable variety of homoatomic (and other) bonding types is found in anionic states of the post-transition metals, and that a great number of these diverse species can be understood in terms of stoichiometry, geometry, and electron count by simple applications of the Zintl-Klemm concepts together with, for electron-deficient deltahedra, the essence of Wade's rules. A great deal of room remains for further investigations that range from exploratory syntheses through property studies and theoretical explanations of the considerable variety of new and unprecedented materials. The greatest experimental difficulty in property measurements is handling these very sensitive phases as they are characteristically strong reducing agents and are readily oxidized to the p-metals. A good deal of attention to the detailed electronic and bonding states of these unusual compounds is needed. For instance, understanding bond length variations and differences in these compounds requires detailed calculations, while very few investigations of stability factors have included the important Madelung energy terms. Their boundaries with metallic and intermetallic substances are in much need of characterization, explanation, and understanding.

As for lessons learned, the more or less new, diverse, and important ways in which electron-poor cluster systems may be stabilized are as follows: 1) distortions of conventional clusters to new bonding regimes; 2) centering of at least main-group elements within clusters; 3) cluster oxidation and formation of cluster networks; 4) utilization of sizable Madelung energy gains in the neat solid state from charged cations that are in intimate contact with anionic clusters or networks; and 5) the serendipitous location of particularly favorable component ions and clusters to achieve very stable three-dimensional structures, a process that at present is only accomplished empirically through synthetic explorations. Opportunities clearly abound!

I am greatly indebted to the outstanding group of graduate and postdoctoral co-workers who have contributed so much to the discoveries described herein and whose names appear in the references, and to the colleagues elsewhere who have volunteered new information in advance of publication. This research was supported by the Office of the Basic Energy Sciences, Materials Sciences Division, US Department of Energy. The Ames Laboratory is operated for the DOE by Iowa State University under Contract No. W-7405-Eng-82.

Received: August 30, 1999 [A 360]

[1] A. Simon, *Struct. Bonding (Berlin)* **1979**, *36*, 81; A. Simon, *Chem. Unserer Zeit* **1988**, *22*, 1.
[2] C. Kittel, *Introduction to Solid State Physics*, 2nd ed., Wiley, New York, NY, **1956**, p. 293.
[3] G. J. Miller in ref. [11], chap. 1.
[4] K. Wade, *Adv. Inorg. Chem. Radiochem.* **1976**, *18*, 1.
[5] J. D. Corbett, *Inorg. Chem.* **1968**, *7*, 198.
[6] F. Laves, *Naturwissenschaften* **1941**, *29*, 244.
[7] W. Klemm, E. Busmann, *Z. Anorg. Allg. Chem.* **1963**, *319*, 297.
[8] H. Schäfer, B. Eisenmann, W. Müller, *Angew. Chem.* **1973**, *85*, 742; *Angew. Chem. Int. Ed. Engl.* **1973**, *12*, 694.
[9] Review: H. Schäfer, *Annu. Rev. Mater. Sci.* **1985**, *15*, 1.
[10] R. Nesper, *Prog. Solid State Chem.* **1990**, *20*, 1.
[11] *Chemistry, Structure and Bonding of Zintl Phases and Ions* (Ed.: S. M. Kauzlarich), VCH, New York, NY, **1996**.
[12] J. D. Corbett, *Chem. Rev.* **1985**, *85*, 383.
[13] H.-D. Hardt, *Die periodischen Eigenschaften der chemische Elemente*, 2nd ed., Georg Thieme, Stuttgart, **1987**, p. 129.
[14] E. Zintl, *Angew. Chem.* **1939**, *52*, 1.
[15] D. G. Adolphson, J. D. Corbett, D. J. Merryman, *J. Am. Chem. Soc.* **1976**, *98*, 7234.
[16] J. D. Corbett in ref. [11], chap. 3, p. 170.
[17] L. Diehl, K. Khodadedeh, D. Kummer, J. Strähle, *Chem. Ber.* **1976**, *109*, 3404.
[18] S. C. Critchlow, J. D. Corbett, *Inorg. Chem.* **1984**, *23*, 770.
[19] A. Cisar, J. D. Corbett, *Inorg. Chem.* **1977**, *16*, 2482.
[20] S. C. Critchlow, J. D. Corbett, *Inorg. Chem.* **1982**, *21*, 3286.
[21] S. C. Critchlow, J. D. Corbett, *Inorg. Chem.* **1985**, *24*, 979.
[22] L. Xu, S. C. Sevov, *J. Am. Chem. Soc.* **1999**, *121*, 9245.
[23] P. A. Edwards, J. D. Corbett, *Inorg. Chem.* **1977**, *16*, 903.
[24] J. Campbell, G. Schrobilgen, *Inorg. Chem.* **1997**, *36*, 4078.
[25] C. Downie, Z. Tang, A. M. Guloy, *Inorg. Chem.*, submitted.
[26] C. H. E. Belin, J. D. Corbett, A. Cisar, *J. Am. Chem. Soc.* **1977**, *99*, 7163.
[27] V. Angilella, C. H. E. Belin, *J. Chem. Soc. Faraday Trans.* **1991**, *87*, 203.
[28] T. F. Fässler, M. Hunziker, *Inorg. Chem.* **1994**, *33*, 5380.
[29] T. F. Fässler, U. Schütz, *Inorg. Chem.* **1999**, *38*, 1866.
[30] S. C. Critchlow, J. D. Corbett, *J. Am. Chem. Soc.* **1983**, *105*, 5715.
[31] T. F. Fässler, M. Hunziker, *Z. Anorg. Allg. Chem.* **1996**, *622*, 837.
[32] J. D. Corbett, P. A. Edwards, *J. Am. Chem. Soc.* **1977**, *99*, 3313.
[33] R. C. Burns, J. D. Corbett, *Inorg. Chem.* **1985**, *24*, 1489.

[34] J. Campbell, D. A. Dixon, H. P. Mercier, G. J. Schrobilgen, *Inorg. Chem.* **1995**, *34*, 5798.
[35] R. C. Burns, J. D. Corbett, *J. Am. Chem. Soc.* **1982**, *104*, 2804.
[36] C. H. E. Belin, H. Mercier, V. Angilella, *New J. Chem.* **1991**, *15*, 931.
[37] D. M. P. Mingos, D. J. Wales, *Introduction to Cluster Chemistry*, Prentice-Hall, Englewood Cliffs, NJ, **1990**.
[38] T. F. Fässler, M. Hunziker, M. E. Spahr, H. Lueken, H. Schilder, *Z. Anorg. Allg. Chem.*, in press.
[39] a) T. F. Fässler, R. Hoffmann, *Chimia* **1998**, *52*, 158; b) T. F. Fässler, R. Hoffmann, *Angew. Chem.* **1999**, *111*, 526; *Angew. Chem. Int. Ed.* **1999**, *38*, 543; c) T. F. Fässler, R. Hoffmann, *J. Chem. Soc. Dalton Trans.* **1999**, 3339.
[40] D. J. Prince, J. D. Corbett, B. Garbisch, *Inorg. Chem.* **1970**, *9*, 2731.
[41] T. W. Couch, D. A. Lokken, J. D. Corbett, *Inorg. Chem.* **1972**, *11*, 357.
[42] J. D. Corbett, *Prog. Inorg. Chem.* **1976**, *21*, 129.
[43] B. Krebs, M. Mummert, C. Brendel, *J. Less-Common Met.* **1986**, *116*, 159.
[44] B. Krebs, M. Hucke, C. J. Brendel, *Angew. Chem.* **1982**, *94*, 453; *Angew. Chem. Int. Ed. Engl.* **1982**, *21*, 445.
[45] R. M. Friedman, J. D. Corbett, *Inorg. Chem.* **1973**, *12*, 1134.
[46] G. Cardinal, R. J. Gillespie, J. F. Sawyer, J. E. Vekris, *J. Chem. Soc. Dalton Trans.* **1982**, 765.
[47] M. E. O'Neill, K. Wade, *J. Mol. Struct.* **1983**, *103*, 259.
[48] H. Schäfer, K. H. Janzon, A. Weiss, *Angew. Chem.* **1963**, *75*, 451; *Angew. Chem. Int. Ed. Engl.* **1963**, *2*, 393.
[49] B. Huang, J. D. Corbett, *Solid State Sci.* **1999**, *1*, 555.
[50] W. Blase, G. Cordier, *Z. Kristallogr.* **1990**, *193*, 319.
[51] V. Quéneau, E. Todorov, S. C. Sevov, *J. Am. Chem. Soc.* **1998**, *120*, 3263.
[52] V. Quéneau, E. Todorov, S. Sevov, unpublished results.
[53] V. Quéneau, S. C. Sevov, *Angew. Chem.* **1997**, *109*, 1842; *Angew. Chem. Int. Ed. Engl.* **1997**, *36*, 1754.
[54] E. Todorov, S. C. Sevov, *Inorg. Chem.* **1998**, *37*, 3889.
[55] V. Quéneau, S. C. Sevov, *Inorg. Chem.* **1998**, *37*, 1358.
[56] M. Klem, J. D. Corbett, unpublished results.
[57] V. Quéneau, S. C. Sevov, *J. Am. Chem. Soc.* **1997**, *119*, 8109.
[58] E. Todorov, S. C. Sevov, *Angew. Chem.* **1999**, *111*, 1892; *Angew. Chem. Int. Ed.* **1999**, *38*, 1775.
[59] A. Hershaft, J. D. Corbett, *Inorg. Chem.* **1963**, *2*, 979.
[60] M. Somer, W. Carrillo-Cabrera, E. M. Peters, K. Peters, H.-G. von Schnering, *Z. Anorg. Allg. Chem.* **1998**, *624*, 1915.
[61] H.-G. von Schnering, M. Bartinger, U. Bolle, W. Carrello-Cabrera, J. Curda, Y. Grin, F. Heinemann, J. Llanos, K. Peters, A. Schmeding, M. Somer, *Z. Anorg. Allg. Chem.* **1997**, *623*, 1037.
[62] E. Todorov, S. C. Sevov, unpublished results.
[63] R. C. Burns, J. D. Corbett, *J. Am. Chem. Soc.* **1981**, *103*, 2627.
[64] U. Zachwieja, J. Müller, J. Włodarski, *Z. Anorg. Allg. Chem.* **1998**, *624*, 853.
[65] D.-P. Huang, J. D. Corbett, *Inorg. Chem.* **1998**, *37*, 5007.
[66] R. Nesper, *Angew. Chem.* **1991**, *103*, 806; *Angew. Chem. Int. Ed. Engl.* **1991**, *30*, 789.
[67] J. F. Smith, D. A. Hansen, *Acta Crystallogr.* **1967**, *22*, 836.
[68] S. C. Sevov, J. D. Corbett, *J. Solid State Chem.* **1993**, *103*, 114.
[69] S. C. Sevov, J. D. Corbett, *Inorg. Chem.* **1991**, *30*, 4875.
[70] W. Blase, G. Cordier, M. Somer, *Z. Kristallogr.* **1991**, *194*, 150.
[71] W. Blase, G. Cordier, V. Müller, U. Häussermann, R. Nesper, *Z. Naturforsch. B* **1993**, *48*, 754.
[72] C. H. E. Belin, M. Tillard-Charbonnel, *Prog. Solid State Chem.* **1993**, *22*, 59.
[73] a) U. Frank-Cordier, G. Cordier, H. Schäfer, *Z. Naturforsch. B* **1982**, *37*, 119; b) F. Cordier, G. Cordier, H. Schäfer, *Z. Naturforsch. B* **1982**, *37*, 127.
[74] C. H. E. Belin, R. G. Ling, *J. Solid State Chem.* **1983**, *48*, 40.
[75] Z.-C. Dong, J. D. Corbett, *Inorg. Chem.* **1996**, *35*, 3107.
[76] Z.-C. Dong, J. D. Corbett, *J. Am. Chem. Soc.* **1994**, *116*, 3429.
[77] D.-P. Huang, J. D. Corbett, *Inorg. Chem.* **1999**, *38*, 316.
[78] J.-T. Zhao, J. D. Corbett, *Inorg. Chem.* **1995**, *34*, 378.
[79] R. Henning, E. A. Leon-Escamilla, J.-T. Zhao, J. D. Corbett, *Inorg. Chem.* **1997**, *36*, 1282.
[80] Z.-C. Dong, J. D. Corbett, *Angew. Chem.* **1996**, *108*, 1073; *Angew. Chem. Int. Ed. Engl.* **1996**, *35*, 1006.
[81] M. L. Fornasini, M. Pani, *J. Alloys Compd.* **1994**, *205*, 179.
[82] B. Huang, J. D. Corbett, *Inorg. Chem.* **1998**, *37*, 1892.
[83] E. A. Leon-Escamilla, J. D. Corbett, *J. Alloys Compd.* **1998**, *265*, 104.
[84] J. D. Corbett, *J. Alloys Compd.* **1995**, *229*, 10.
[85] Z.-C. Dong, J. D. Corbett, *J. Am. Chem. Soc.* **1993**, *115*, 11299.
[86] Z.-C. Dong, J. D. Corbett, *Inorg. Chem.* **1996**, *35*, 2301.
[87] D.-P. Huang, Z.-C. Dong, J. D. Corbett, *Inorg. Chem.* **1998**, *37*, 5881.
[88] S. Kaskel, J. D. Corbett, *Inorg. Chem.* **2000**, in press.
[89] R. W. Henning, J. D. Corbett, *Inorg. Chem.* **1997**, *36*, 6045.
[90] Z.-C. Dong, J. D. Corbett, *J. Cluster Sci.* **1995**, *6*, 187.
[91] Z.-C. Dong, J. D. Corbett, *Inorg. Chem.* **1996**, *35*, 1444.
[92] Z.-C. Dong, J. D. Corbett, *Inorg. Chem.* **1995**, *34*, 5042.
[93] S. C. Sevov, J. D. Corbett, J. E. Ostenson, *J. Alloys Compd.* **1993**, *202*, 289.
[94] S. C. Sevov, J. D. Corbett, *Inorg. Chem.* **1993**, *32*, 1059.
[95] Z.-C. Dong, R. Henning, J. D. Corbett, *Inorg. Chem.* **1997**, *36*, 3559.
[96] R. W. Henning, J. D. Corbett, *Inorg. Chem.* **1999**, *38*, 3883.
[97] S. C. Sevov, J. D. Corbett, *J. Am. Chem. Soc.* **1993**, *115*, 9089.
[98] Z.-C. Dong, J. D. Corbett, unpublished results.
[99] Z.-C. Dong, J. D. Corbett, *J. Am. Chem. Soc.* **1995**, *117*, 6447.
[100] Z.-C. Dong, J. D. Corbett, *Inorg. Chem.* **1995**, *34*, 5709.
[101] H.-J. Meyer, R. Hoffmann, *J. Solid State Chem.* **1991**, *95*, 14.
[102] Y. Tiang, T. Hughbanks, *Inorg. Chem.* **1993**, *32*, 400.
[103] G. Cordier, V. Müller, *Z. Naturforsch. B* **1994**, *49*, 935.
[104] M. M. Tillard-Charbonnel, C. H. E. Belin, A. P. Manteghetti, D. M. Flot, *Inorg. Chem.* **1996**, *35*, 2583.
[105] S. C. Sevov, J. D. Corbett, *Inorg. Chem.* **1993**, *32*, 1612.
[106] W. Carrillo-Cabrera, N. Caroca-Canales, H.-G. von Schnering, *Z. Anorg. Allg. Chem.* **1994**, *620*, 247.
[107] C. H. E. Belin, M. Tillard-Charbonnel, *Coord. Chem. Rev.* **1998**, *178–180*, 529.
[108] B. Eisenmann, G. Cordier in ref. [11], sect. 2.09.
[109] W. van der Lugt in *Chemistry, Structure and Bonding of Zintl Phases and Ions* (Ed.: S. M. Kauzlarich), VCH, New York, NY, **1996**, chap. 4.
[110] S. A. van der Aart, P. Verkerk, Y. S. Dadyai, W. van der Lugt, *J. Chem. Phys.* **1998**, *108*, 9214.
[111] T. Hughbanks in *Inorganometallic Chemistry* (Ed.: T. Fehlner), Plenum, New York, NY, **1992**, p. 291.
[112] H.-G. von Schnering, *Nova Acta Leopold.* **1985**, *59*, 168.
[113] J.-T. Zhao, J. Corbett, *Inorg. Chem.* **1994**, *33*, 5721.
[114] a) R. Kröner, K. Peters, H.-G. von Schnering, R. Nesper, *Z. Kristallogr. New Cryst. Struct.* **1998**, *213*, 667; b) R. Kröner, K. Peters, H.-G. von Schnering, R. Nesper, *Z. Kristallogr. New Cryst. Struct.* **1998**, *213*, 669; c) R. Kröner, K. Peters, H.-G. von Schnering, R. Nesper, *Z. Kristallogr. New Cryst. Struct.* **1998**, *213*, 671; d) R. Kröner, K. Peters, H.-G. von Schnering, R. Nesper, *Z. Kristallogr. New Cryst. Struct.* **1998**, *213*, 675.
[115] B. Eisenmann, H. Schäfer, R. Zagler, *J. Less-Common Met.* **1996**, *118*, 43.
[116] J. T. Vaughey, J. D. Corbett, *J. Am. Chem. Soc.* **1996**, *118*, 12103.
[117] W. Blase, G. Cordier, R. Kniep, R. Schmidt, *Z. Naturforsch. B* **1989**, *44*, 505.
[118] A. K. Ganguli, A. M. Guloy, E. A. Leon-Escamilla, J. D. Corbett, *Inorg. Chem.* **1993**, *32*, 1351.
[119] J. T. Vaughey, J. D. Corbett, *Inorg. Chem.* **1997**, *36*, 4316.
[120] *Binary Alloy Phase Diagrams*, 2nd ed. (Eds.: T. B. Massalski), ASM International, Materials Park, OH, **1990**.
[121] E. Zintl, W. Dullenkopf, *Z. Phys. Chem.* **1932**, *16B*, 183.
[122] H.-G. von Schnering, *Angew. Chem.* **1981**, *93*, 44; *Angew. Chem. Int. Ed. Engl.* **1981**, *20*, 33.
[123] P. C. Schmidt, *Struct. Bonding (Berlin)* **1987**, *65*, 91.
[124] S. C. Sevov, J. D. Corbett, *Z. Anorg. Allg. Chem.* **1993**, *619*, 128.
[125] M. Tillard-Charbonnel, C. H. E. Belin, J. L. Soubeyroux, *Eur. J. Solid State Inorg. Chem.* **1990**, *27*, 759.
[126] C. H. E. Belin, *Acta Crystallogr. Sect. B* **1980**, *36*, 1339.
[127] R. G. Ling, C. H. E. Belin, *Z. Anorg. Allg. Chem.* **1981**, *480*, 1981.
[128] W. Blase, G. Cordier, *Z. Naturforsch. B* **1989**, *44*, 479.
[129] W. Blase, G. Cordier, *Z. Naturforsch. B* **1989**, *44*, 1011.
[130] G. Cordier, V. Müller, *Z. Naturforsch. B* **1995**, *50*, 23.
[131] D. M. Flot, M. M. Tillard-Charbonnel, C. H. E. Belin, *J. Am. Chem. Soc.* **1996**, *118*, 5229.
[132] S. C. Sevov, J. D. Corbett, *Inorg. Chem.* **1992**, *31*, 1895.
[133] S. Kaskel, J. D. Corbett, *Inorg. Chem.*, submitted.

[134] S. C. Sevov, J. D. Corbett, *Science* **1993**, *262*, 880.
[135] S. C. Sevov, J. D. Corbett, *J. Solid State Chem.* **1996**, *123*, 344.
[136] J. T. Vaughey, J. G. Harp, J. D. Corbett, unpublished results.
[137] G. Cordier, H. Schäfer, M. Stelter, *Z. Anorg. Allg. Chem.* **1986**, *539*, 33.
[138] R. Nesper, private communication.
[139] D.-K. Seo, J. D. Corbett, unpublished results.
[140] E. A. Leon-Escamilla, J. D. Corbett, unpublished results.
[141] N. N. Greenwood, A. Earnshaw, *Chemistry of the Elements*, 2nd ed., Butterworth-Heinemann, Oxford, UK, **1997**, p. 222.
[142] B. Huang, J. D. Corbett, *Inorg. Chem.* **1998**, *37*, 5827.
[143] K. J. Nordell, G. J. Miller, *Inorg. Chem.* **1999**, *38*, 579.
[144] M. Tillard-Charbonnel, A. Chahine, C. H. E. Belin, R. Rousseau, E. Canadell, *Eur. J. Chem.* **1997**, *3*, 799.
[145] J. K. Burdett, E. Canadell, *Inorg. Chem.* **1991**, *30*, 1991.